CHAPTER III

RESULTS AND DISCUSSION

3.1 Enantiomeric Separation Using Single Cyclodextrin

3.1.1 BGE Conditions

AP, MA, PE, EP and NE are basic compounds (Figure 1.13) with pK_a values of 10.1, 9.87, 10.3, 10.3 and 9.44, respectively. Therefore, a background electrolyte at acidic pH was selected to allow separation of the enantiomers as positively charged compounds. Typically, CZE separation of basic enantiomers is performed using a phosphate buffer at pH 2.5 to 3.0. In previous work, enantiomeric separation of AP, MA, EP and NE was carried out in the phosphate buffer at pH 2.5 using tris(hydroxymethyl)aminomethane ($trisH^+$) as a BGE co-ion [Cheryl *et al.* 1995]. In this work, a triethanolammonium-phosphate buffer at pH 3.0 was chosen. The use of the low pH phosphate buffer with triethanolamine to adjust the pH has been shown to have the advantageous effects of preventing wall interactions for cationic analytes and giving good peak symmetry [Bechet *et al.* 1994]. Protonated triethanolamine has been shown to provide better resolution than a conventional buffer cation such as $trisH^+$ and Na^+. This may be explained, using Equations 1.20 to 1.21, by the fact that worse resolution using Na^+ and $trisH^+$ as the BGE co-ion is partly due to the greater EMD resulted from their higher electrophoretic mobility (μ^o = $+5.3 \times 10^{-8}$, $+2.95 \times 10^{-8}$ and $+2.85 \times 10^{-8}$ $m^2\ V^{-1}\ s^{-1}$ for Na^+, $trisH^+$ and triethanolammonium, respectively [Pospichal *et al.* 1989 and Foret *et al.* 1993]. Therefore, Na^+ and $trisH^+$ give greater mobility difference than triethanolammonium with typical basic analytes in the presence of CD ($a_A \propto 1 - \mu_A/\mu_C$, when $\mu_C > \mu_A$ in Equation 3.11). In addition, the triethanolammonium-phosphate buffer has usefulness for suppressing EOF [Fillet *et al.* 1995] due to the binding of triethanolammonium cations to negatively charged ionize silanol sites on the capillary walls. Using the triethanolammonium-phosphate buffer, Ferguson *et al.* [1996] reported that EOF was less

than 0.11 x 10^{-8} m^2 V^{-1} s^{-1}. Erny [2002] reported that, at low pH BGE, the extra EMD of analytes caused by H_3O^+ is significant when the ratio of the concentration of H_3O^+ to that of the BGE co-ion is greater than 1/20. In this study, the BGE used was prepared by titrating 0.10 M H_3PO_4 with triethanolamine to pH 3.0, giving ionic strength of 0.088 mol kg^{-1} or M. Altria *et al.* [1992] suggested that a BGE co-ion concentration at least 100 times greater than analyte is essential in order to reduce EMD and to prevent analyte wall interaction. However, the higher the BGE concentration, the greater the heat generation. The BGE used in this experiment has been previously used for separation of basic enantiomers [Bechet *et al.* 1994, Ferguson *et al.* 1996, Ferguson *et al.* 1997 and Nhujak 2001].

3.1.2 Binding Constant and Enantioselectivity

Simultaneuos separation of AP, MA, PE, EP and NE enantiomers in single CD was carried out as a procedure described in Section 2.3. Figures 3.1 and 3.2 show examples of electropherograms for separation of these enantiomers with separate β-CD and DM-β-CD, respectively. From Figure 3.1a, five peaks are observed due to no separation of each pair of enantiomers. By spiking standard analytes, the migrating enantiomers were found to be AP, MA, PE, EP and NE at migration times of 7.00, 7.23, 7.78, 7.86 and 8.03 min, respectively, indicating the order of electrophoretic mobility (μ) AP > MA > NE > PE > EP. The greatest μ for AP is possibly due to the smallest size (Figure 1.13 and $\mu \propto z/r_h$ as shown in Equation 1.6). The smaller μ for PE, EP and NE may be due to intra-hydrogen bonding in a molecule, resulting in a decrease in effective charge, z. The smallest μ for EP may be caused by either the less effective charge or larger size.

It is seen from Figure 3.1 that resolution of each pair of AP, MA, PE and EP enantiomers was acheived using β-CD as a chiral selector, while no enantiomeric resolution of NE was obtained with β-CD over its full solubility range (0-16 mM). From Figure 3.2 enantiomeric resolution of each pair of enantiomers, except for AP where $R_s < 1.5$, was achieved using DM-β-CD as a chiral selector. However, baseline resolution for simultaneous separation of all five enantiomers using β-CD or DM-β-CD was not achieved ($R_s < 1.5$). It should be noted that each peak was identified by spiking standard analytes and comparing with previous work [Cheryl *et al.* 1995].

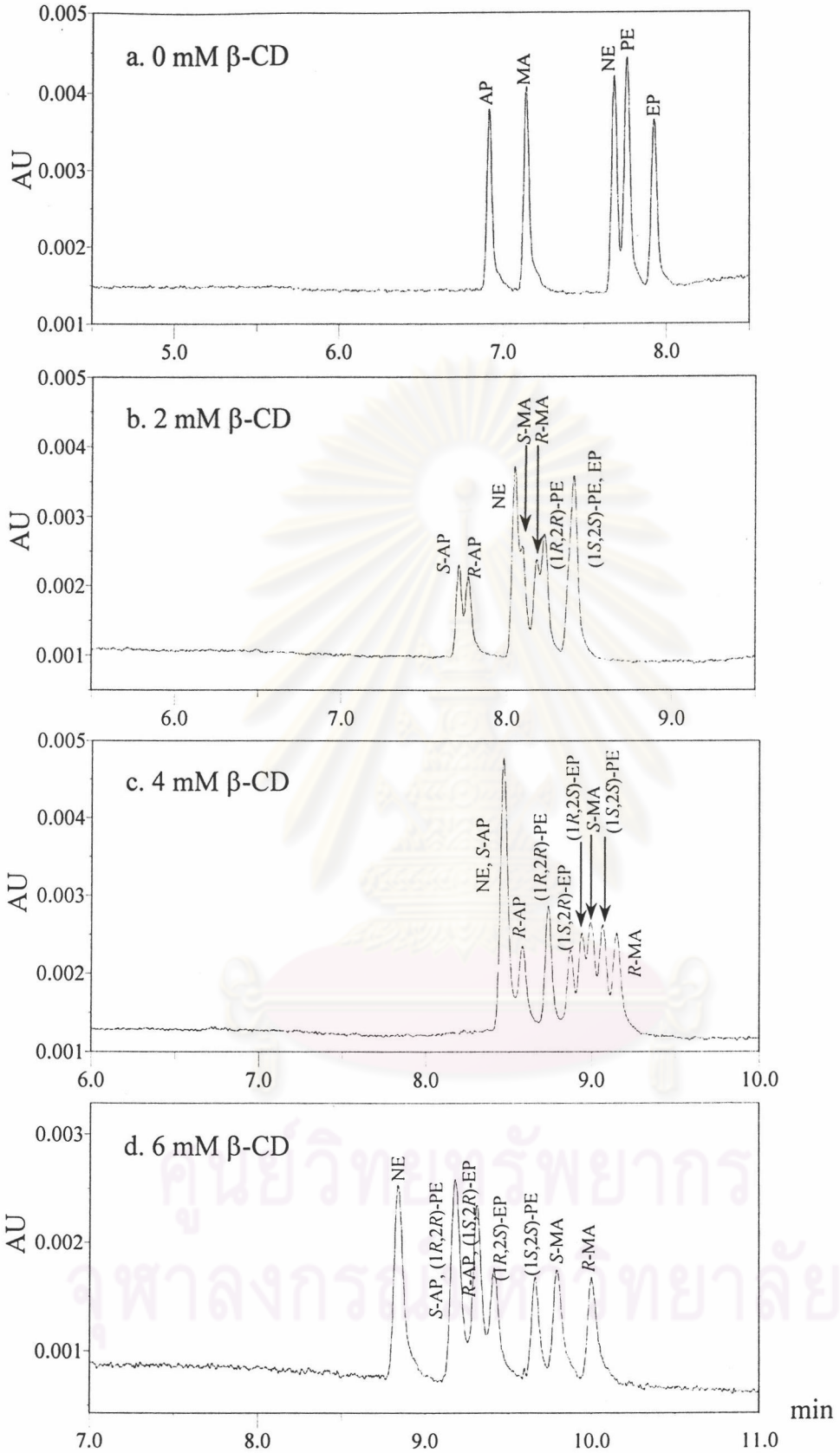

Figure 3.1 Electropherograms of enantiomeric separation of AP, MA, PE, EP and NE using β-CD as chiral selector. CE conditions: uncoated fused silica 50 μm i.d. × 57 cm (50 cm to detector), temperature 25 °C, BGE as 100 mM phosphoric acid titrated to pH 3.0 with triethanolamine, voltage 30 kV, 0.5 psi pressure injection for 2 s and UV detection at 200 nm.

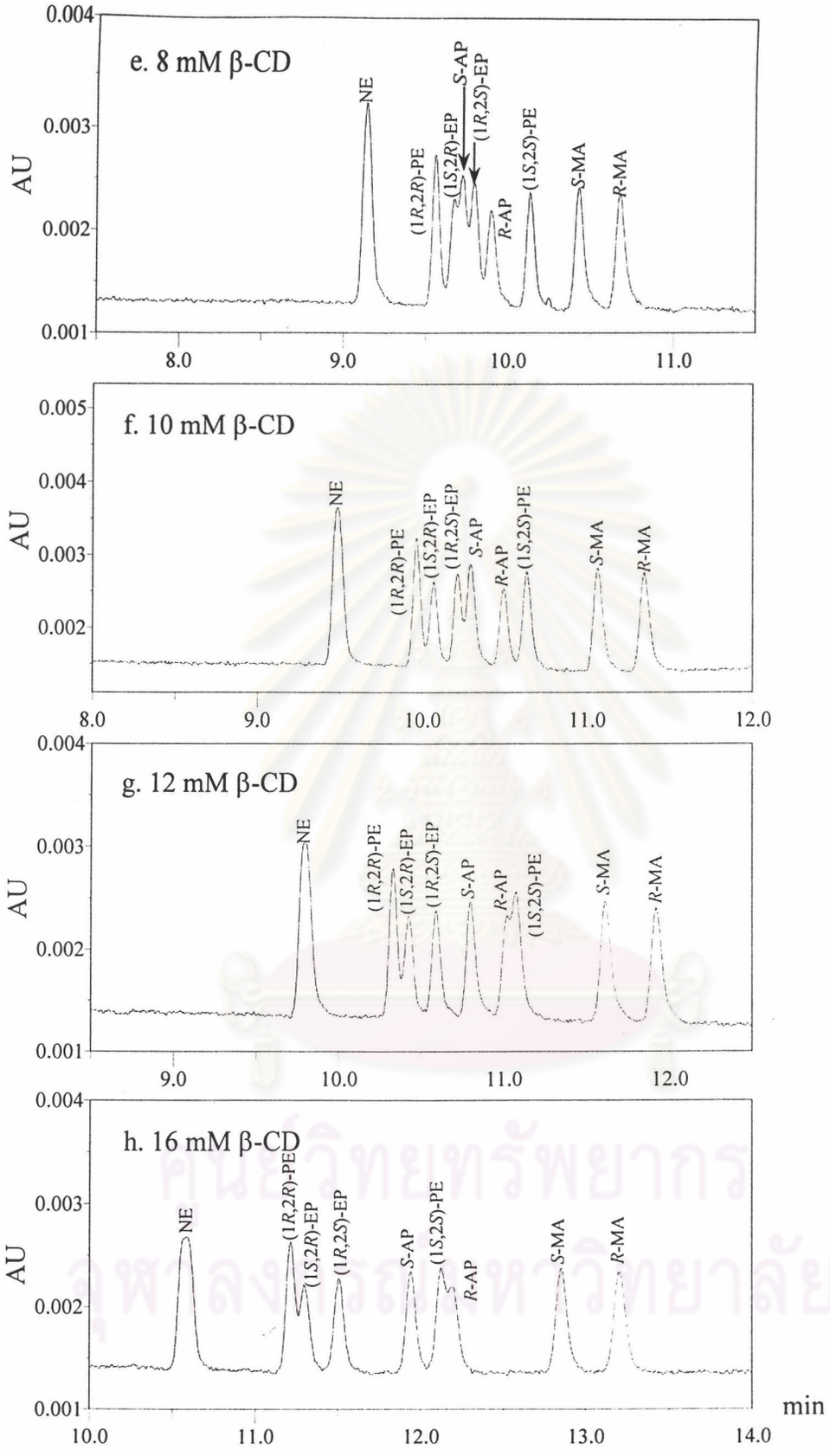

Figure 3.1 Continued.

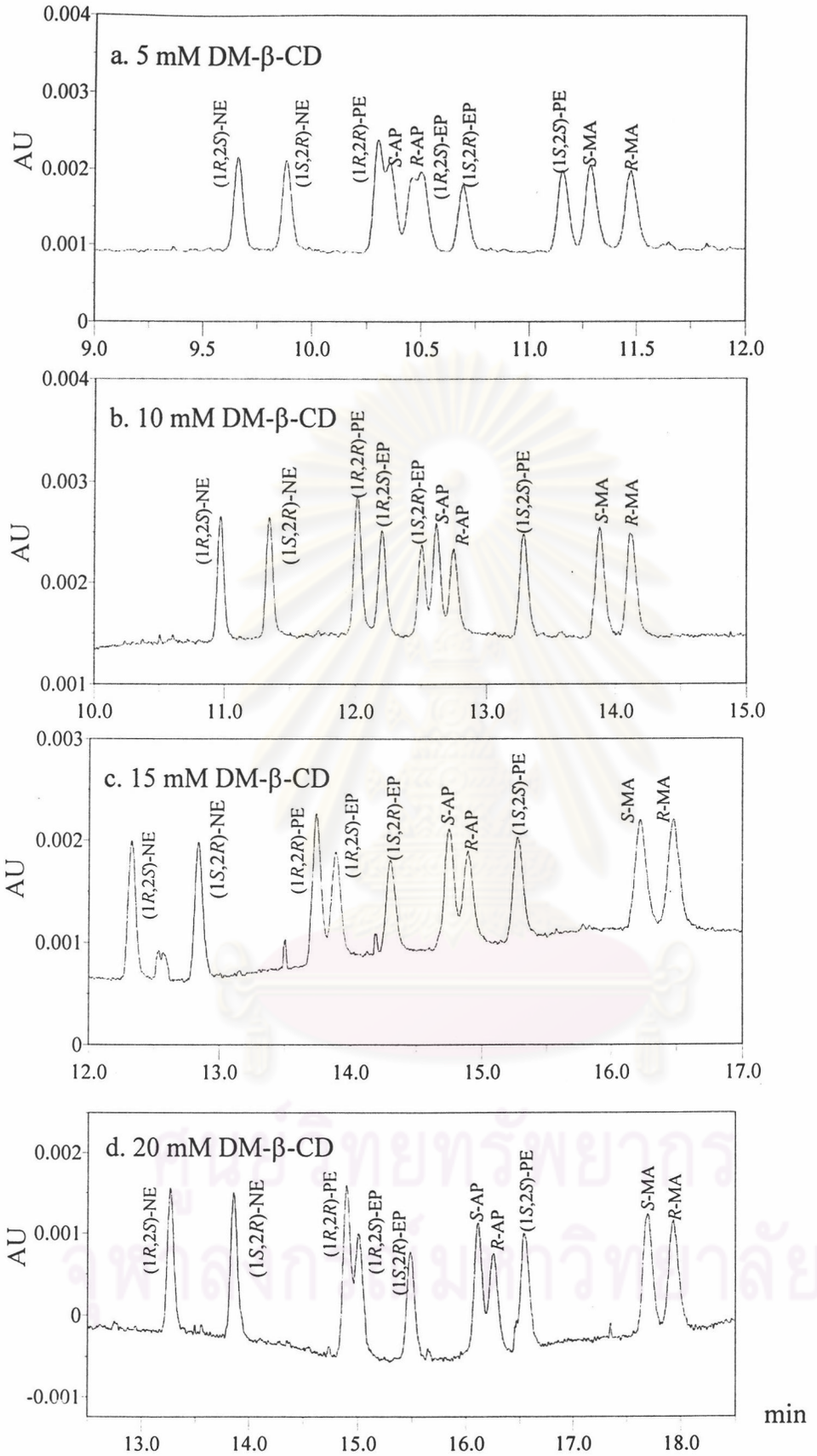

Figure 3.2 Electropherograms of enantiomeric separation of AP, MA, PE, EP and NE using DM-β-CD as chiral selector. CE conditions as shown in Figure 3.1.

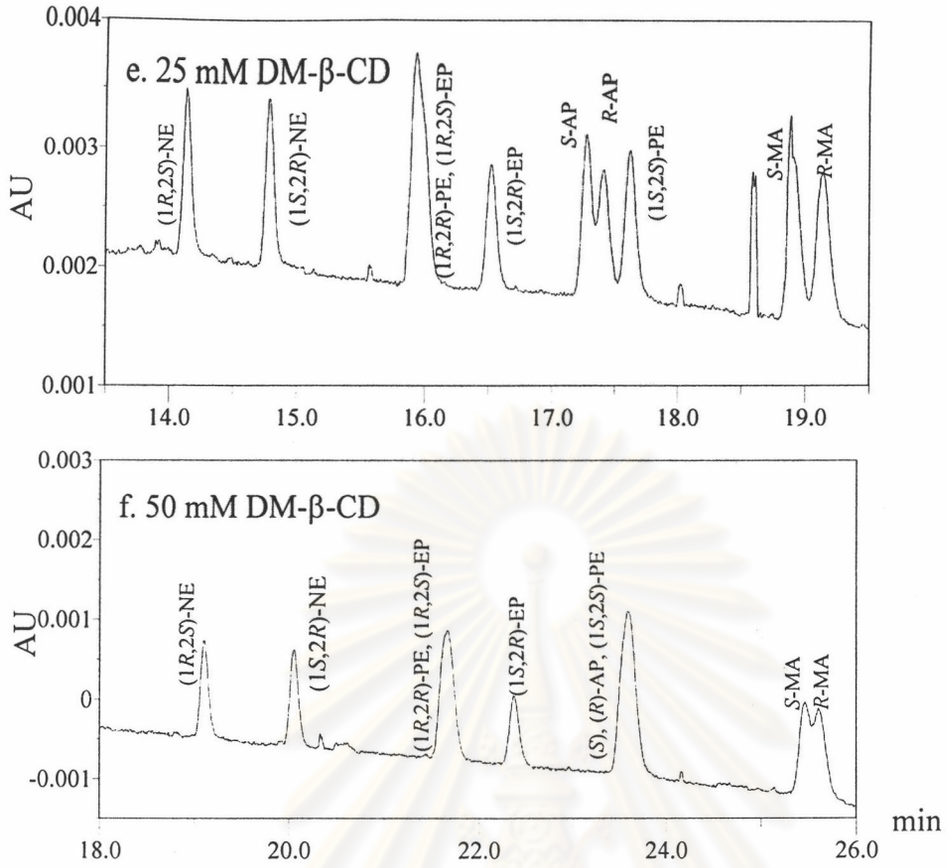

Figure 3.2 Continued.

To compare theory and practice in enantiomeric resolution, the binding constants for each enantiomer to CD were determined in order to predict electrophoretic mobility difference, peak variance and resolution. At a given CD concentration, the observed and corrected electrophoretic mobility (μ_{obs} and μ) were obtained as previously mentioned in Section 2.3. The relationship between corrected electrophoretic mobility and the concentration of β-CD and DM-β-CD is shown in Figure 3.3. Each of the μ values was measured as the mean of two runs. Binding constant and electrophoretic mobility of CD inclusion complexes as shown in Table 3.1 were obtained from Equation 1.33 and the CEfit program of a non-linear least-squares fit to the data points [Penn *et al.* 1995 and Rudick 1997]. From the binding constants, it can be concluded that the binding strength is in order MA > AP > PE > EP > NE. The smaller binding constants for PE, EP and NE are possibly due to an additional hydroxy group of enantiomers, resulting in a decrease in the hydrophobic interaction between the analyte and CD. Compared with β-CD, DM-β-CD shows the stronger binding with each enantiomer. This may be due to the additional hydrophobic interactions between the phenyl group and the cavity as the methylated groups of DM-β-CD. It should be noted that DM-β-CD is a β-CD derivative in which the hydroxy groups at positions 2 and 6 in each glucose units are methylated.

From Table 3.1, the binding strength was in order, *R*- > *S*- isomer for AP and MA to β-CD and DM-β-CD, (1*R*,2*R*) > (1*S*,2*S*) isomer for PE to β-CD and DM-β-CD. Therefore, no change in migration order was observed for AP, MA and PE enantiomers using β-CD or DM-β-CD as chiral selector. For EP, the strong binding was in order (1*R*,2*S*) > (1*S*,2*R*) isomer for β-CD, while (1*R*,2*S*) < (1*S*,2*R*) isomer for DM-β-CD. Therefore, the migration order of EP enantiomers was opposite when using β-CD or DM-β-CD. The binding constants for NE enantiomers to β-CD were found to be equal, thus no separation of enantiomers was obtained.

(a) β-CD

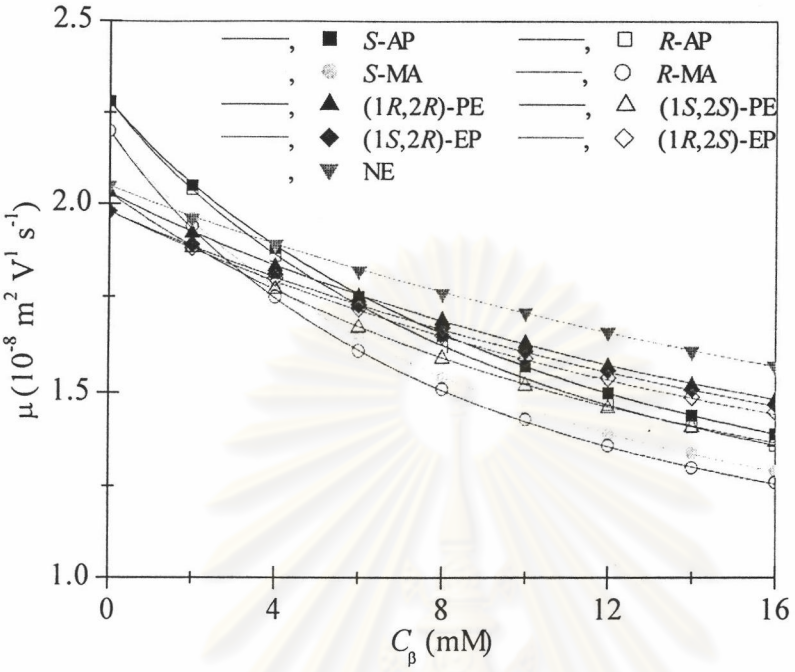

(b) DM-β-CD

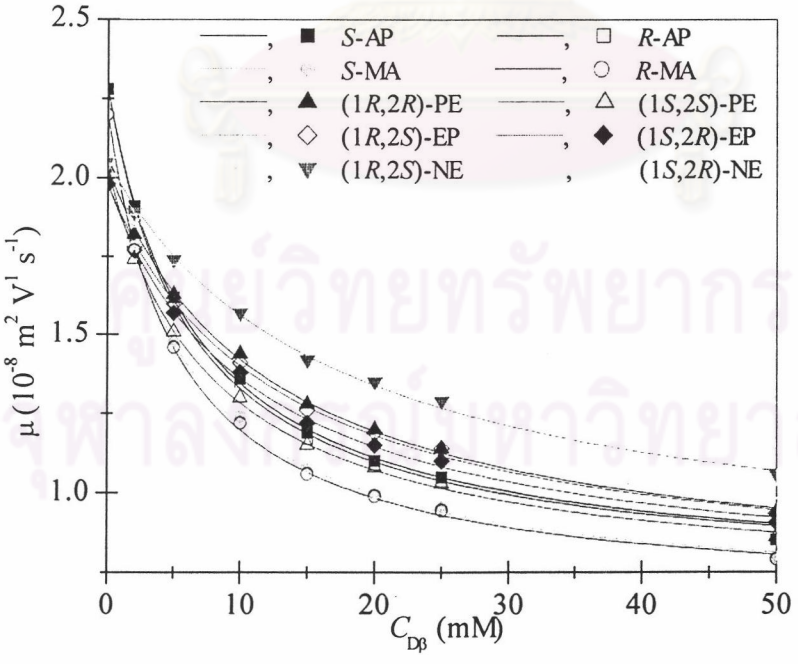

Figure 3.3 Binding curves for AP, MA, PE, EP and NE enantiomers to (a) β-CD and (b) DM-β-CD. Experimental (symbols) μ is the average of two runs and corrected with BGE viscosity as Equation 2.2. Predicted (solid lines) μ is obtained from Equation 2.5 and data in Table 3.1.

Table 3.1 Binding constants, electrophoretic mobilities and enantioselectivity for AP, MA, PE, EP and NE

CD	analytes	K/M^{-1}				$\mu/10^{-8}\ m^2s^{-1}V^{-1}$		α
		first migration		second migration		μ_o	μ_∞	
β-CD	AP	K_S	85.46 ± 0.58	K_R	92.71 ± 0.66	2.28 ± 0.01	0.74 ± 0.01	1.085
	MA	K_S	99.83 ± 0.59	K_R	110.10 ± 0.65	2.20 ± 0.01	0.72 ± 0.01	1.103
	PE	$K_{1R,2R}$	42.03 ± 0.34	$K_{1S,2S}$	59.37 ± 0.47	2.03 ± 0.01	0.67 ± 0.01	1.413
	EP	$K_{1S,2R}$	36.31 ± 0.20	$K_{1R,2S}$	38.90 ± 0.18	1.98 ± 0.01	0.58 ± 0.01	1.071
	NE	$K_{1R,2S}$	29.75 ± 0.30	$K_{1S,2R}$	29.75 ± 0.30	2.05 ± 0.01	0.56 ± 0.01	1.000
DM-β-CD	AP	K_S	149.6 ± 2.6	K_R	156.4 ± 2.6	2.28 ± 0.01	0.72 ± 0.01	1.045
	MA	K_S	176.6 ± 3.4	K_R	185.7 ± 3.2	2.20 ± 0.01	0.66 ± 0.01	1.052
	PE	$K_{1R,2R}$	83.9 ± 1.5	$K_{1S,2S}$	127.2 ± 2.4	2.03 ± 0.01	0.70 ± 0.01	1.516
	EP	$K_{1R,2S}$	82.3 ± 1.7	$K_{1S,2R}$	92.9 ± 1.6	1.98 ± 0.01	0.70 ± 0.01	1.129*
	NE	$K_{1R,2S}$	59.1 ± 1.2	$K_{1S,2R}$	70.2 ± 1.2	2.05 ± 0.01	0.74 ± 0.01	1.187

K and μ_∞ are obtained from a non-linear fit of data point of μ as a function of C using Equation 1.33 and a CE fitting program of K. *$K_{1R,2S}/K_{1S,2R}$ of EP = 0.886

Enantioselectivity, α, is defined as the ratio of the binding constant, K_j/K_i, where $K_j > K_i$ [Penn *et al.* 1994]. In this case, *i* and *j* refer to the first and the second migration order. $\alpha = 1$ indicates no enantiomeric resolution, such as NE enantiomers with β-CD. The greater the enantioselectivity, the higher the enantiomeric resolution. The α values in Table 3.1 suggested that β-CD give higher optimum resolution of AP and MA enantiomers than does DM-β-CD, while DM-β-CD gives higher optimum resolution of PE, EP and NE enantiomers than does β-CD. However, CD concentration at maximum resolution depends on binding constant. Further discussion is present in Section 3.1.3. The enantioselectivity cannot be predicted easily. It depends on analytes and CD types, and does not relate to the binding strength.

3.1.3 CD Concentrations at Maximum Electrophoretic Mobility Difference and Maximum Resolution

Figure 3.4 shows a comparison of observed and predicted values of electrophoretic mobility difference ($\Delta\mu$), corrected with relative viscosity, over a wide range of CD concentrations. At a given CD concentration, the predicted $\Delta\mu$ was obtained from Equation 1.34 using data of ΔK, $\bar{K}$, μ_o and μ_∞ in Table 3.1. From plots of $\Delta\mu$ as a function of C in Figure 3.4, the predicted $\Delta\mu$ increases with an increase of C up to maximum, then falls off gradually. Good agreement was obtained between observed and predicted $\Delta\mu$ over a wide range of CD concentrations. The CD concentration at maximum $\Delta\mu$ ($C_{\Delta\mu,max}$) may be calculated from Equation 1.34 by using differential calculus. At $d\Delta\mu/dC = 0$, maximum $\Delta\mu$ occurs when [Wren and Rowe 1992a and Penn *et al.* 1993, 1994]

$$C_{\Delta\mu,max} = \frac{1}{\bar{K}} \qquad (3.1)$$

From Table 3.2, the observed and predicted CD concentrations at $\Delta\mu$ maximum were found to be in good agreement. Equation 3.1 indicates that the higher the binding constant, the lower the CD concentration at maximum $\Delta\mu$. This can be used to explain the difference in $C_{\Delta\mu,max}$ for each pair of enantiomers as shown in Figure 3.4 and Table 3.2. For each pair of enantiomers, the lower $C_{\Delta\mu,max}$ was obtained for DM-β-CD than β-CD due to the greater binding constant for DM-β-CD as a reason previously mentioned in Section 3.1.2.

(a) β-CD

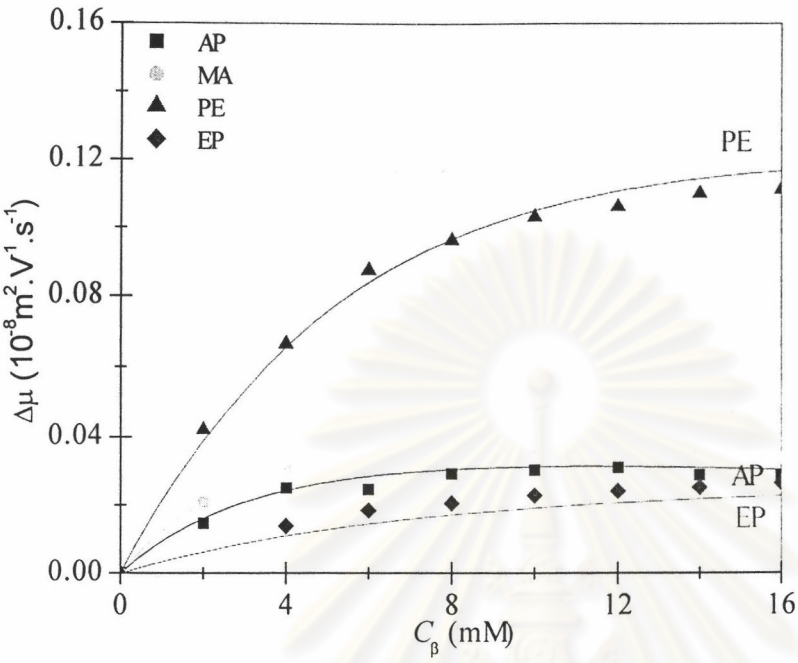

(b) DM-β-CD

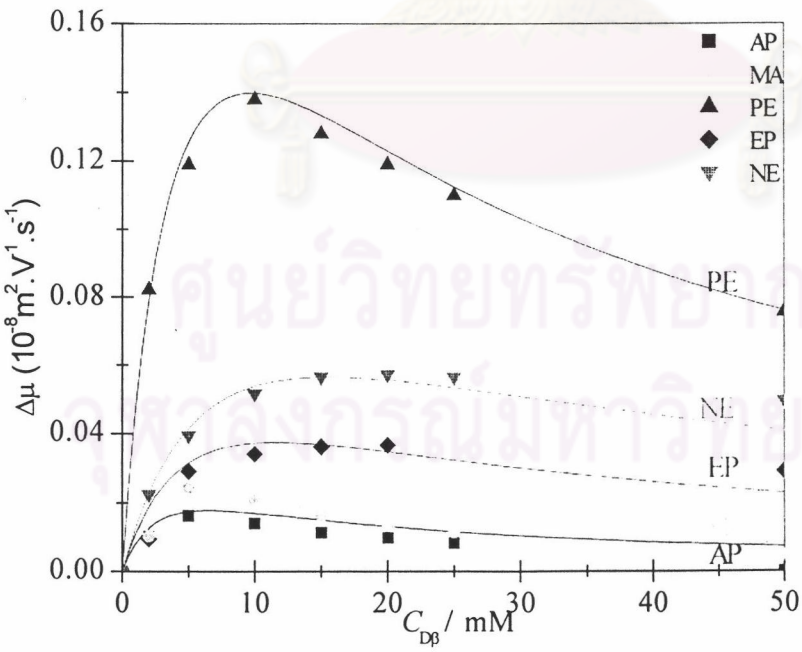

Figure 3.4 Electrophoretic mobility difference (Δμ) for each pair of AP, MA, PE, EP and NE enantiomers using (a) β-CD and (b) DM-β-CD. Experimental Δμ (symbol) is the average for two runs and corrected with the BGE viscosity using Equation 2.2. Predicted Δμ (solid line) is obtained using Equation 1.34 and data in Table 3.1.

Table 3.2 Calculated and observed CD concentration at maximum Δμ and maximum R_s using β-CD and DM-β-CD as a chiral selector

	analytes	at $\Delta\mu_{max}$/mM		at $R_{s,max}$/mM	
		[a]$C_{calc,\Delta\mu max}$	C_{obs}	[b]$C_{calc,Rsmax}$	C_{obs}
β–CD	AP	11.2	10.0-14.0	19.7	>16.0*
	MA	9.5	8.0-10.0	16.7	>16.0*
	PE	20.0	>16.0*	34.8	>16.0*
	EP	26.6	>16.0*	49.2	>16.0*
	NE[c]	no resolution	no resolution	no resolution	no resolution
DM-β-CD	AP	6.5	5.0-10.0	11.6	10.0-15.0
	MA	5.5	5.0	10.1	5.0-10.0
	PE	9.7	10.0	16.5	15.0-20.0
	EP	11.4	10.0-20.0	19.3	20.0-25.0
	NE	15.5	15.0-25.0	25.9	25.0-50.0

*maximum solubility of β–CD
[a]observed using Equation 3.1 and data in Table 3.1
[b]observed using Equation 3.3 and data in Table 3.1
[c]no resolution of NE enantiomers.

When peak variance due only to diffusion is taken into account, it follows from Equations 1.14, 1.33 and 1.34 that enantiomric resolution is equal to the equation

$$R_s = \frac{\Delta\mu}{4\sqrt{2}}\sqrt{\frac{Vl}{L\bar{D}\left(\bar{\mu}+\mu_{eo}\right)}} \qquad (3.2)$$

when $\mu_{eo} = 0$ and μ_o for $\bar{D}$ in Equation 1.17 is assumed to be equal to $\bar{\mu}$, differentiation of Equation 3.2 with respect to $\bar{K}C$ gives the CD concentration at maximum resolution ($C_{R_s,max}$) [Penn *et al.* 1994]

$$C_{R_s,max} = \frac{1}{\bar{K}}\sqrt{\frac{\mu_o}{\mu_\infty}} \qquad (3.3)$$

Using Equation 3.3 and data in Table 3.1, the predicted concentration at maximum resolution $C_{Rs,max}$ is shown in Table 3.2. The observed values of enantiomeric resolution in a wide range of CD concentrations are shown in Figure 3.8, obtained from measuring

peak width at base and using Equation 1.13. From Figure 3.8 and Table 3.2, the observed and predicted $C_{Rs,max}$ were found to be in good agreement. Both experiment and prediction show that CD concentration at maximum R_s is slightly greater than CD concentration at maximum $\Delta\mu$. From prediction, the value of (μ_o/μ_∞) is always greater than 1.0. Therefore, in the absence of EOF, it follows from Equations 3.1 and 3.2 that the predicted $C_{Rs,max} = (\mu_o/\mu_\infty)^{1/2}/\bar{K}$ is greater than $C_{\Delta\mu,max} = 1/\bar{K}$. This is because peak resolution is proportional to $\Delta\mu/\sqrt{\mu}$ (Equation 1.14), and μ decreases with increasing CD concentration. This favors CD concentration higher than $C_{\Delta\mu,max}$ [Nhujak 2001]. It should be noted that the solubility of β-CD is in the range of 0 to 16 mM. Therefore, the maximum $\Delta\mu$ and R_s were not observed for PE and EP using β-CD as selector, due to $\bar{K}$ < 62.5 M^{-1}.

3.1.4 Observed and Predicted Peak Variance and Peak Efficiency

3.1.4.1 Predicted Peak Variance

Details of peak broadening in CE were previously discussed in Section 1.2.4. Two major contributions, longitudinal diffusion and electromigration dispersion, were taken into account for prediction of peak variance. Other contributions, such as detection aperture width, detector time constant and injection length after sample stacking, are negligible, each less than 0.1×10^{-7} m^2. Thermal dispersion and analyte wall absorption are difficult to predict. Nhujak [2001] derived equations involving peak variance due to longitudinal diffusion (σ^2_{diff}) and electromigration dispersion (σ^2_{EMD}) as a function of the dimensionless quantity *KC*.

Firstly, peak variance due to longitudinal diffusion is considered. In the absence of EOF, it follows Equations 1.16, 1.17, 1.33 and 2.2 that the value of σ^2_{diff} may be calculated using the equation [Nhujak 2001]

$$\sigma^2_{diff} = \frac{2kTlL}{zeV}\left(\frac{\frac{\mu^o_o}{\mu^o_\infty}+KC}{\frac{\mu_o}{\mu_\infty}+KC}\right)\frac{\mu^o_\infty}{\mu_\infty} \qquad (3.8)$$

where μ^o_o and μ^o_∞ are the electrophoretic mobilities of the fully charged analyte and its complex, respectively, at zero ionic strength of the BGE. In the case of a univalent analyte in the uni-univalent BGE at 25 °C, μ^o_o and μ^o_∞ may be calculated using the equation given by Survay *et al.* [1996]

$$\mu = \mu^o - \left(0.229\mu^o + 3.12\times10^{-8}\frac{\sqrt{I}}{1+3.28a\sqrt{I}}\right) \qquad (3.9)$$

where I is the ionic strength of BGE ($I = 1/2\Sigma C_i z_i^2$) and a (in nm) the sum hydrodynamic radii of the analyte ion and counter ion. The hydrodynamic radius (r_h) is previously given in Equation 1.6, and μ^o is used instead of μ. Electrophoretic mobilities of analytes and BGE ions at zero and experimental ionic strength are shown in Table 3.3.

Table 3.3 Electrophoretic mobilities at zero and experimental ionic strength

ions	Electrophoretic mobility ($\times 10^{-8}$ $m^2V^{-1}s^{-1}$)					
	free analyte		analyte:CD complex			
			β-CD		DM- β-CD	
	μ_o	μ_o^o	μ_∞	μ_∞^o	μ_∞	μ_∞^o
AP	2.28[a]	3.00[a]	0.74[a]	1.24[a]	0.67[a]	1.16[a]
MA	2.20[a]	2.91[a]	0.72[a]	1.22[a]	0.66[a]	1.14[a]
PE	2.03[a]	2.72[a]	0.67[a]	1.16[a]	0.70[a]	1.19[a]
EP	1.98[a]	2.66[a]	0.58[a]	1.04[a]	0.68[a]	1.17[a]
NE	2.05[a]	2.74[a]	0.56[a]	1.02[a]	0.74[a]	1.24[a]
$H_2PO_4^-$	-2.85[b]	-3.41[c]	-	-	-	-
triethanolammonium	2.15[b]	2.85[c]	-	-	-	-

[a]Obtained from experiment (Table 3.1)
[b]Calculated using Equation 3.9 and I = 0.088 mol kg^{-1}
[c]Obtained from Pospeichal *et al.* 1989 and Foret *et al.* 1993

Next, peak variance due to EMD is discussed. In the absence of EOF, it follows from Equation 1.20 that the value of σ^2_{EMD} may be calculated using the equation

$$\sigma^2_{EMD} = \left| \frac{2}{9} l l_{inj} c_A a_A \right| \tag{3.10}$$

For Equation 3.10, each parameter is defined as in Equations 1.20 and 1.21. A change in viscosity due to CD affects a change of observed electrophoretic mobilities of both analyte and BGE ions. However, the observed mobility ratio used in Equation 1.21 for calculation of a_A is equal to the corrected mobility ratio, e.g. $\mu_{A,obs}/\mu_{C,obs} = \mu_A/\mu_C$. In this case at I = 0.088 mol kg^{-1}, μ_A refers to the net electrophoretic mobility of analyte and its complex (μ in Equation 1.33). μ_B and μ_C refer to the electrophoretic mobilities of $H_2PO_4^-$ and triethanolammonium, respectively. From Equation 1.33, the value of μ_A/μ_C in Equation 1.21 is related to the dimensionless quantity KC as the equation [Nhujak 2001]

$$\frac{\mu_A}{\mu_C} = \left(\frac{\frac{\mu_o}{\mu_\infty} + KC}{1 + KC} \right) \frac{\mu_\infty}{\mu_C} \tag{3.11}$$

The predicted values of σ^2_{diff}, σ^2_{EMD} and total peak variance (σ^2_{tot}), shown in Figure 3.5, are the average for two enantiomers. Therefore, $\overline{KC}$ is used in Equations 3.8 and 3.11. From Equations 3.8, 3.10 and 3.11, at a fixed CD concentration, the predicted values of σ^2_{diff} for each type of enantiomers are slightly different due to slight difference in the mobility ratios of μ^o_∞/μ_∞ and the value in the blanket in Equation 3.8. In a wide range of CD concentrations, the predicted values of σ^2_{diff} for each type of enantiomers slightly increase with increasing CD concentration. From Equation 3.8, when other parameters are constant, the value of σ^2_{diff} depends on KC. At $C = 0$ and $C = \infty$, the values of σ^2_{diff} are equal to $f_{diff}\mu^o_o/\mu_o$ and $f_{diff}\mu^o_\infty/\mu_\infty$, respectively, where $f_{diff} = 2kTlL/zeV$ [Nhujak 2001]. For example, the value of μ^o_o/μ_o = 1.32 and μ^o_∞/μ_∞ = 1.69 for MA, therefore, the predicted values of σ^2_{diff} increase 28 % from $C = 0$ to $C = \infty$.

With increasing CD concentration, the predicted values of σ^2_{EMD} in Figure 3.5 increase to maximum, and is seem to decrease if the CD concentration is greater than experimental concentration used in this work. From Equations 1.20 and 3.10, σ^2_{EMD} is related to l_{inj} and a_A. In our experiment, a constant injection time of 2 s was used, and thus l_{inj} decreases with increasing viscosity of the BGE as the concentration of CD increases. However, at the beginning range of CD concentration, a decrease of l_{inj} is less than an increase of a_A, resulting in an increase of $l_{inj} \times a_A$ with increasing CD concentration. At the high concentration of CD, a decrease of l_{inj} is approximate an increase of a_A, resulting in slight difference of $l_{inj} \times a_A$ with increasing CD concentration. In comparison with other analytes, MA is seen to have the greatest value of predicted σ^2_{EMD} due to the strongest binding with CD (Table 3.1) and smallest μ_A (Figure 3.3). This results in the greatest different mobility of analytes and the BGE co-ion, leading to the greatest a_A (Equation 1.21). For each type of enantiomers and equal concentration of β-CD and DM- β-CD, DM-β-CD should give the higher values of predicted σ^2_{EMD} due to the smaller μ_A caused by stronger binding of each analyte and CD. The total peak variance as shown in Figure 3.5 (the upper line) is the sum of σ^2_{diff} and σ^2_{EMD}. The predicted value of total peak variance slightly increases due to a slight increase of σ^2_{diff} and σ^2_{EMD} as previously mentioned.

(a) β-CD

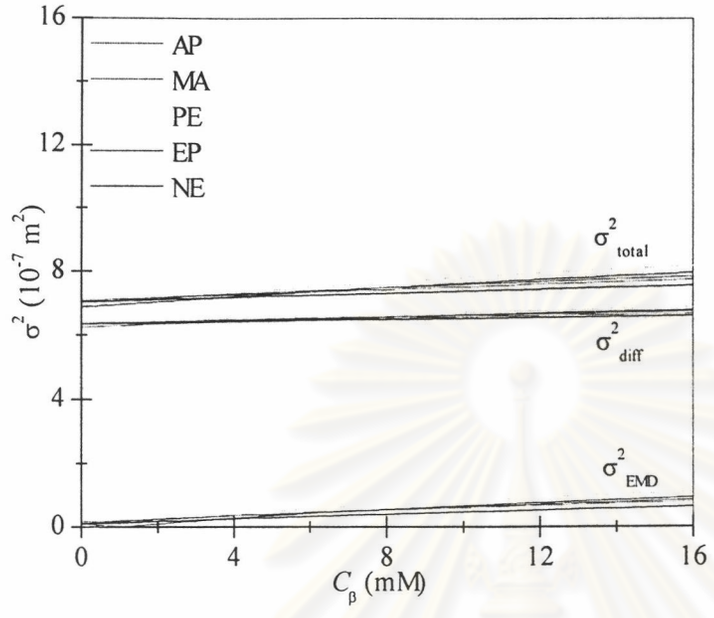

(b) DM-β-CD

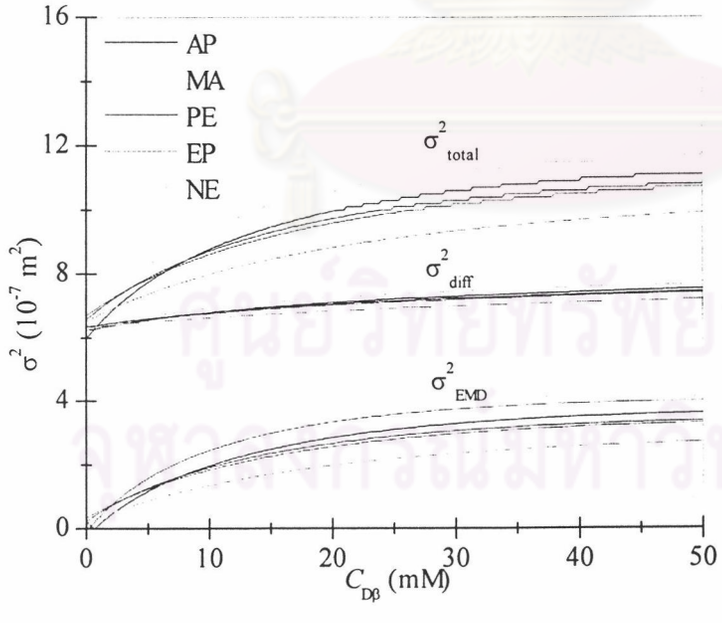

Figure 3.5 Predicted peak variance for AP, MA, PE, EP and NE enantiomers using (a) β-CD and (b) DM-β-CD. σ^2 is the average for each pair of enantiomers. σ^2_{diff} and σ^2_{EMD} are obtained from Equations 3.8 and 3.10, respectively, and data from Tables 3.1 and 3.3.

3.1.4.2 Comparison of Observed and Predicted Total Peak Variance

Observed and predicted values of σ^2_{tot} are compared as shown in Figures 3.6a and 3.6b for using β-CD and DM-β-CD as a chiral selector, respectively. Each predicted value (solid line) of σ^2_{tot} is the average for a pair of enantiomers as previously mentioned in Section 3.1.4.1. The observed value of σ^2_{tot} was obtained from measurement of peak width at base from electropherograms in Figures 3.1 and 3.2, and calculation using Equation 1.9. σ^2_{tot} is equal to $(v\tau)^2$, where $v = l/t_m$. Each observed value is for each isomer. Some observed σ^2_{tot} cannot be determined due to very closed peaks, such as AP, MA and PE at 50.0 mM DM-β-CD. For using β-CD (Figure 3.6a), the observed values of σ^2_{tot} are approximately twice higher than the predicted values for AP, MA, PE and EP, and twice to four times for NE. For using DM-β-CD (Figure 3.6b), the observed values of σ^2_{tot} are approximately 10 to 25 % higher than the predicted values for all test enantiomers. The result of this difference is thought to be other sources, especially analyte-wall absorption and extra EMD. The effect of extra EMD is firstly considered. The parameter c_A for calculation of σ^2_{EMD} in Equations 1.20 and 3.10 is the concentration analyte in the analyte zone, and these equations are valid for a single analyte. For the zone containing multiple analytes, the total concentration of multiple analytes is higher than the single analyte. This results in the observed σ^2_{EMD} greater than the predicted σ^2_{EMD} calculated from Equations 1.20 and 3.10. In this work, it is difficult to predict the extra EMD caused by the overlapping or co-migrating analytes. Next consideration is the effect of analyte-wall adsorption. Since test analytes carry a positive charge, the interaction between analyte and negatively charge capillary wall is possible. In comparison with DM-β-CD, β-CD gave higher difference in the observed and predicted σ^2_{tot} possibly due to the interaction between capillary wall and hydroxy groups of CD encapsulating analyte. It should be noted that β-CD contains 21 hydroxy groups, while 7 hydroxy groups for DM-β-CD. There have been reported that alcohols and carbohydrates, which contain hydroxy groups, can interact with the capillary wall. In comparison with other analytes using β-CD (Figure 3.6b), NE was found to have higher difference in the observed and predicted σ^2_{tot} due to extra EMD caused by co-migration of NE enantiomers. This difference between NE and other analytes was not observed for DM-β-CD (Figure 3.6b).

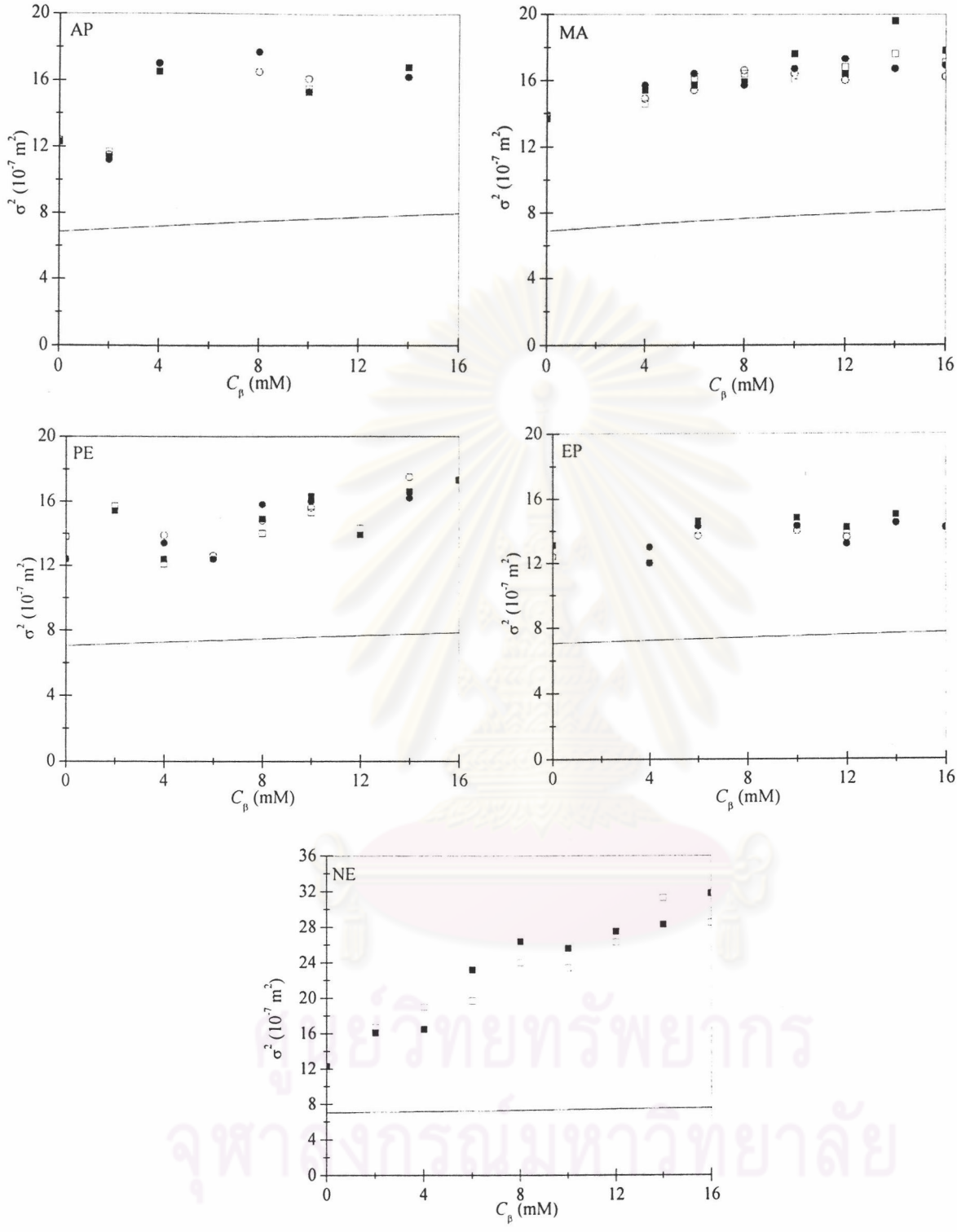

(a) β-CD

Figure 3.6 Observed (symbols) and predicted (solid lines) total peak variance (σ^2_{tot}) for AP, MA, PE, EP and NE enantiomers using (a) β-CD and (b) DM-β-CD. The predicted value is the average for each pair of enantiomers obtain from Figure 3.5a. The observed value is obtained from each isomer for each run. The black and blank symbols refer to the first and second run, respectively.

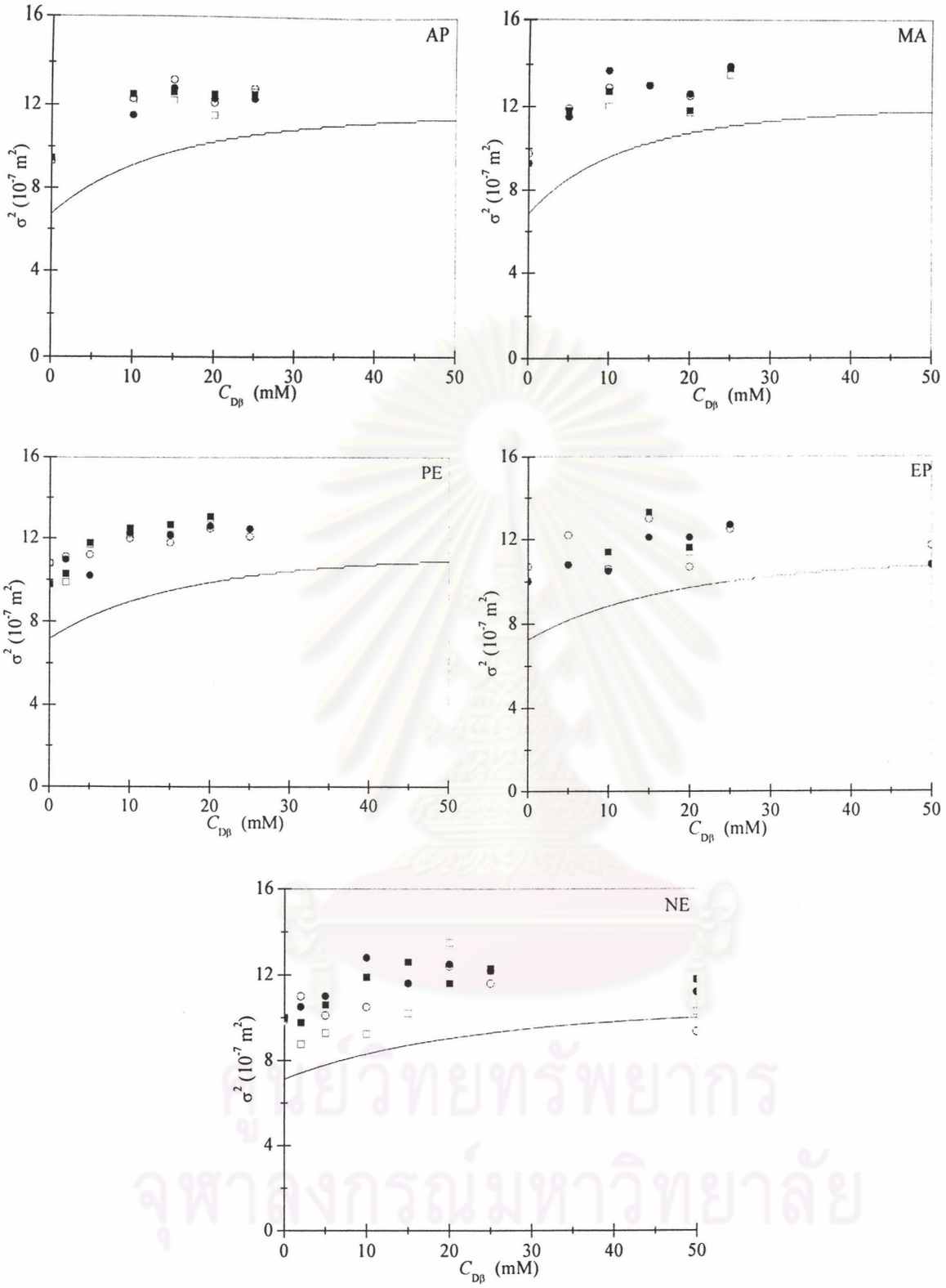

(b) DM-β-CD

Figure 3.6 Continued.

3.1.4.3 Observed and Predicted Peak Efficiency

Figures 3.7 shows a comparison of observed and predicted peak efficiency of each pair of enantiomers using β-CD and DM-β-CD, respectively. The average value of peak efficiency (N) was calculated using Equation 1.12 and data in Figure 3.6. The observed $\bar{N}$ for each pair of enantiomers was obtained from the same run. Over the wide range of CD concentrations used, observed values of $\bar{N}$ were found to be in the range ≈ (1.0 to 2.0) × 10^5 for β-CD and ≈ (1.8 to 2.6) × 10^5 for DM-β-CD, while the predicted values of $\bar{N}$ were in the range ≈ 3.5 × 10^5 for β-CD and ≈ (2.5 to 3.0) × 10^5 for DM-β-CD. Since peak efficiency is proportional to $1/\sigma_{tot}^2$, any difference in the observed and predicted values can be explained in a similar way to peak variance.

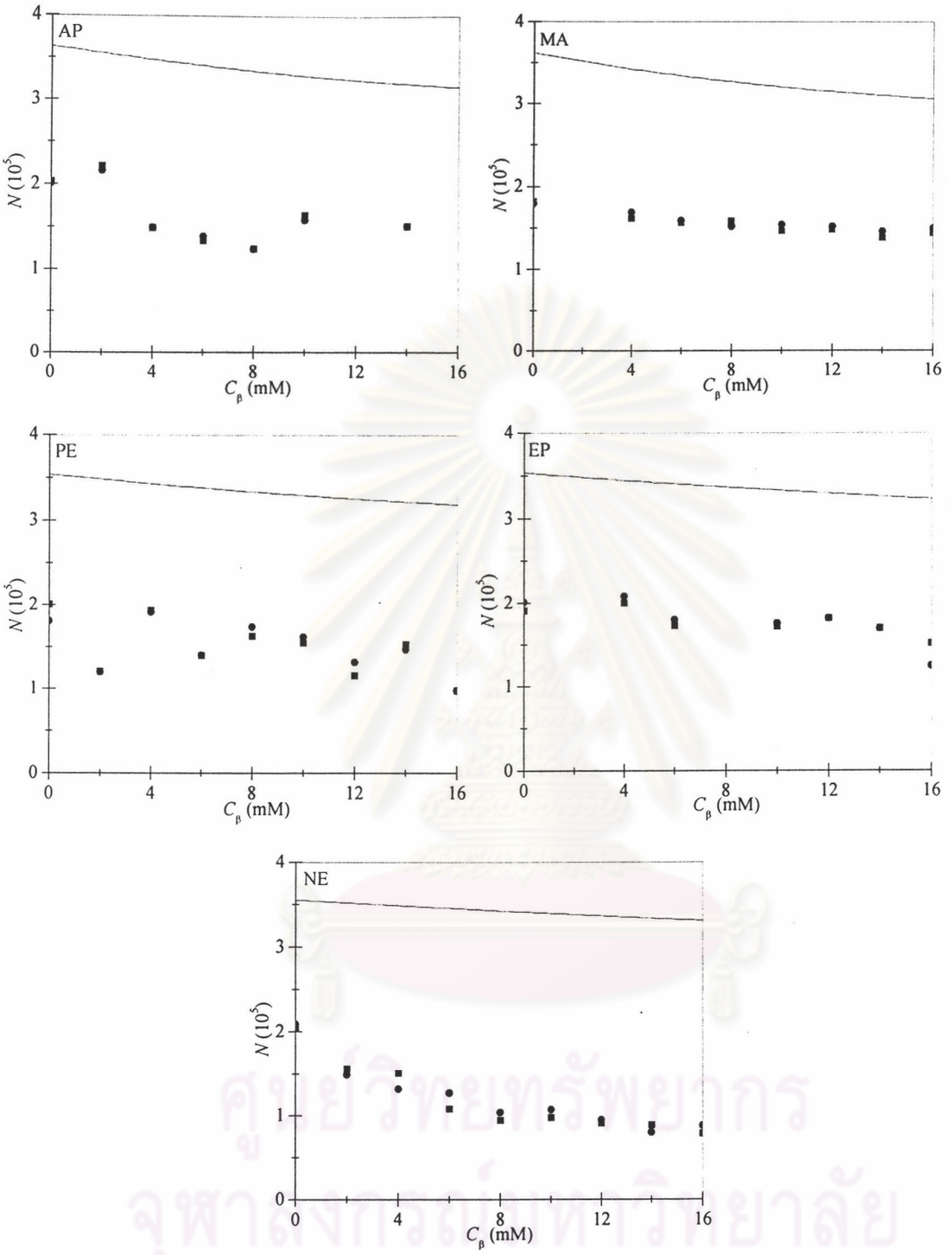

(a) β-CD

Figure 3.7 Observed (symbols) and predicted (solid lines) peak efficiency (*N*) for each pair of AP, MA, PE, EP and NE enantiomers using (a) β-CD and (b) DM-β-CD. Each value is the average for two enantiomers in the same run. ■ and ● refer to the first and second run, respectively.

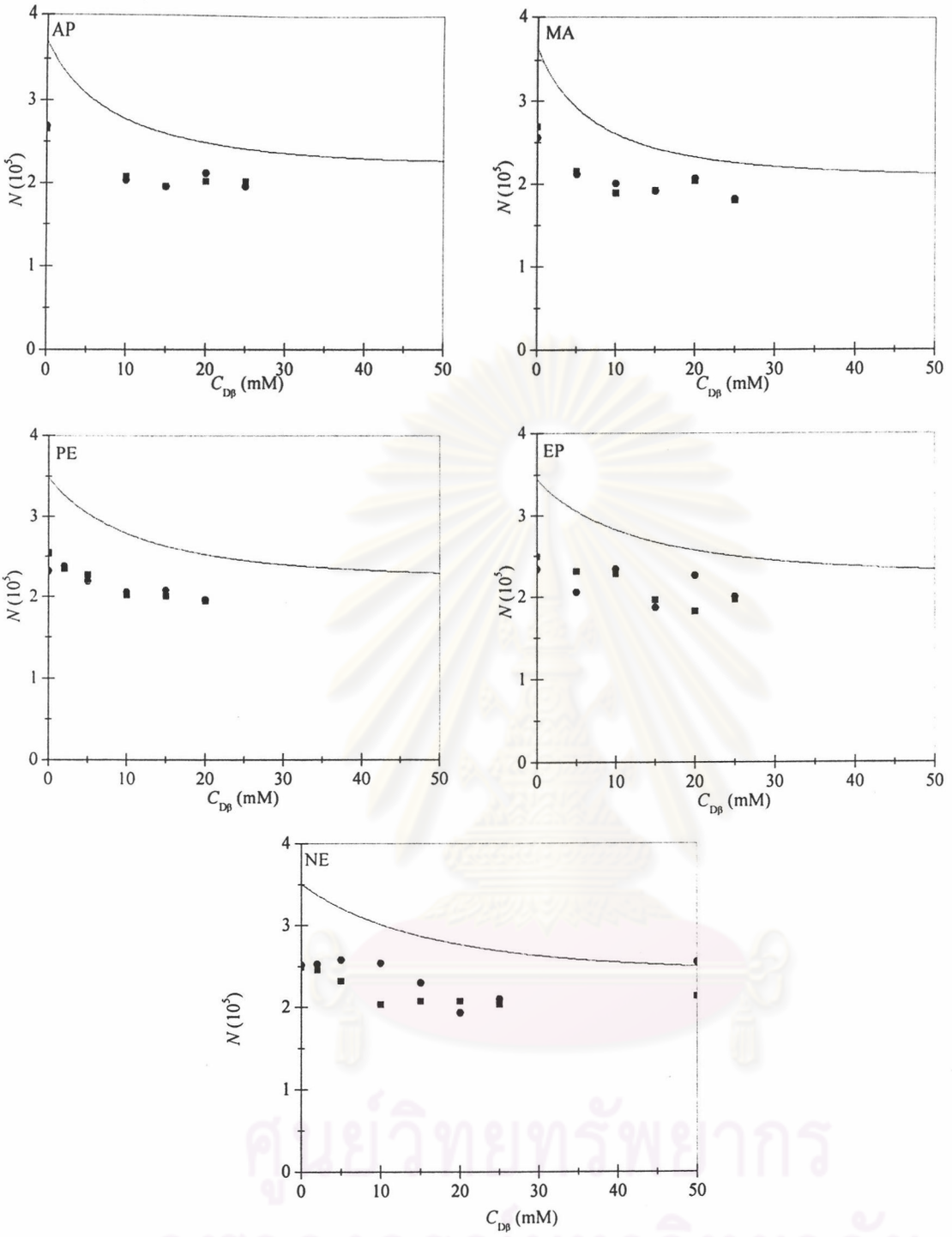

(b) DM-β-CD

Figure 3.7 Continued.

3.1.5 Observed and Predicted Enantiomeric Resolution

Figure 3.8 shows a comparison of the values of observed and predicted resolution over a wide range of CD concentrations. The observed values of R_s were obtained as previously mentioned in Section 3.1.3. In the absence of EOF, resolution in Equation 1.14 is given by

$$R_s = \frac{1}{4}\left(\frac{\Delta\mu}{\bar{\mu}}\right)\sqrt{\bar{N}} \qquad (3.12)$$

The predicted values of R_s were calculated using Equation 3.12 and data of $\bar{\mu}$, $\Delta\mu$ and N from Figures 3.2, 3.3 and 3.7, respectively. Over a wide range of CD concentrations, the observed and predicted values have the same trend. Good agreement between observed and predicted resolution was obtained for all enantiomers using DM-β-CD and EP using β-CD, while the values of observed slightly less than predicted resolution were found for AP, MA and PE using β-CD. The difference in the observed and predicted R_s is due to the difference in $\bar{N}$ as previously mentioned in Section 3.1.4.2 and Figures 3.7a and 3.7b. It should be noted that R_s depends on $\bar{\mu}$, $\Delta\mu$ and $\bar{N}$. However, good agreement between observed and predicted $\bar{\mu}$ and $\Delta\mu$ are obtained in this work.

In previous work on enantiomeric resolution of fenfluramine enantiomers over a wide range of CD concentrations [Nhujak 2001], TM-β-CD gave good agreement between the observed and predicted resolution, while DM-β-CD gave the observed resolution slightly less than did TM-β-CD. At the CD concentration giving maximum resolution, the observed and predicted resolution was obtained to be in good agreement for terbutaline and propanolol using HP-β-CD [Ferguson 1997 and Nhujak 2001], while the observed resolution of tioconazole enantiomers using β-CD was found to be approximately half of the prediction [Ferguson *et al.* 1996]. The observed resolution less than prediction may be due to peak broadening contribution from analytes and capillary wall interaction as discussed in their work [Ferguson *et al.* 1996 and Nhujak 2001].

(a) β-CD

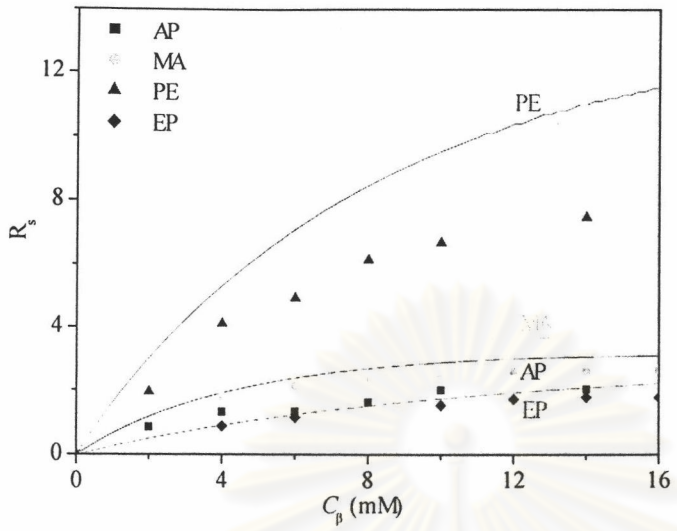

(b) DM-β-C

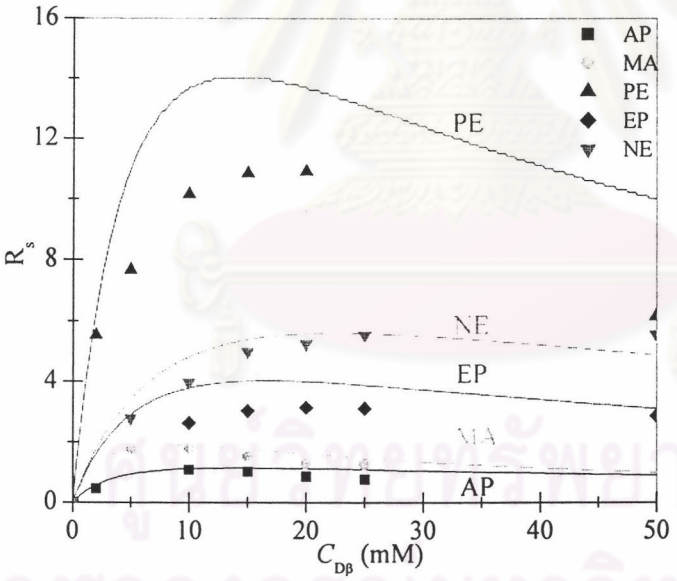

Figure 3.8 Observed (symbols) and predicted (solid lines) resolution (R_s) for each pair of AP, MA, PE, EP and NE enantiomers using (a) β-CD and (b) DM-β-CD. Observed R_s is the average for two runs. Obsreved and predicted values R_s are obtained from Equation 3.12 and data from Figures 3.3, 3.4 and 3.7.

Using CE conditions, as in this experiment for separation of basic compounds, Nhujak [2001] proposed the simple equation $R_s \approx 30(\alpha\text{-}1)$ for the maximum resolution of enantiomers, where α is the enantioselectivity. Table 3.4 shows a comparison of observed and predicted values of maximum resolution.

The values of predicted $R_{s,max}$ from this work in Figure 3.5 are obtained to be in good agreement with the simple equation $R_s \approx 30(\alpha\text{-}1)$. In comparison with predicted $R_{s,max}$ obtained Figure 3.8, the values of observed $R_{s,max}$ are also found to be in good agreement with prediction, except for AP, MA and PE where observed 25-35 % less than predicted $R_{s,max}$ was obtained.

Table 3.4 Predicted and observed values of maximum resolution.

CD	enantiomers	α	predicted $R_{s,max}$		[c]observed $R_{s,max}$
			[a]$R_s \approx 30(\alpha\text{-}1)$	[b]Figure 3.5	
β-CD	AP	1.085	2.6	3.1	2.0
	MA	1.103	3.1	3.7	2.7
	PE	1.413	12.4	11.5	7.5
	EP	1.071	2.1	2.2	1.8
	NE	1.000	0.0	0.0	0.0
DM-β-CD	AP	1.045	1.4	1.3	1.2
	MA	1.052	1.6	1.9	1.9
	PE	1.516	15.5	14.0	12.0
	EP	1.129	3.9	4.0	3.6
	NE	1.187	5.6	5.6	5.8

[a]the equation is obtained from Nhujak [2001]
[b]solid line in Figure 3.7
[c]observed R_s in Figure 3.7

3.1.6 Observed and Predicted Simultaneous Separation of Several Pairs of Enantiomers

For separation of one pair of enantiomers, the optimum CD concentration should be in the range of the CD concentration at maximum $\Delta\mu$ or maximum R_s, in order to achieve high resolution. However, for simultaneous separation of several pairs of enantiomers, the resolution of each pair and different pairs of enantiomers should be considered.

In this section, the values of electrophoretic mobilities of enantiomers from experiment and calculation are considered to compare observed and predicted simultaneous separation of several pair enantiomers. Simultaneous separation of enantiomers using β-CD is firstly discussed. From predicted μ (solid lines) in Figure 3.3a, over a range of β-CD concentrations between 0 to 9 mM, the values of μ for AP, MA and/or PE enantiomers overlapping those of other enantiomers indicate that no achieved resolution of some pairs of analytes ($R_s < 1.5$). For example, at 2.0 mM β-CD, the following pairs have almost identical μ: NE enantiomers:*S*-MA, *R*-MA:*S*-PE and *R*-PE:EP enantiomers, which is in good agreement with the pattern of the observed electropherogram in Figure 3.1b. At 8.0 mM β-CD, μ of *S*-AP is between that of EP enantiomers, therefore closed three peaks are obtained, in good agreement with the pattern of the observed electropherogram in Figure 3.1e. At 11 to 16 mM β-CD in Figures 3.3a and 3.4a, the predicted $\Delta\mu \geq 0.02\times10^{-8}$ $m^2V^{-1}s^{-1}$ is seen for each pair of AP, MA, PE and EP enantiomers, indicating achieved baseline resolution for each pair of enantiomers. However, *R*-AP and (1*S*,2*S*)-PE have almost identical μ, leading to co-migration of these two analytes, which is in good agreement with the electropherogram in Figure 3.1g. For the predicted μ (solid lines) in Figure 3.3a, the suitable β-CD concentration of 10.0 mM is seen for simultaneous separation of AP, MA, PE and EP enantiomers. This is found to be in good agreement with the pattern of the observed electropherogram in Figure 3.1f.

Simultaneous separation using DM-β-CD is now considered. From predicted μ (solid lines) in Figure 3.3b, over a range of DM-β-CD concentrations between 0 to 8 mM, the values of μ for AP and MA enantiomers overlapping those of other enantiomers indicate that no achieved resolution of some pairs of analytes. For example, at 5.0 mM DM-β-CD, the values of μ are almost identical for the following pairs of analytes: (1*R*,2*R*)-PE:*S*-AP

and *R*-AP:(1*S*,2*R*)-EP, indicating co-migration of these pairs of analytes. The observed electropherogram in Figure 3.2a (5.0 mM) is found to be in good agreement with prediction. At above 20.0 mM DM-β-CD in Figure 3.3b, predicted Δμ of (1*R*,2*R*)-PE and (1*R*,2*S*)-EP is seen to decrease with increasing DM-β-CD concentration, indicating an increase of co-migration, which is in good agreement with the observed electropherograms in Figures 3.2d-f. In addition, AP enantiomers at above 20.0 mM DM-β-CD have a decrease in predicted Δμ and their electrophoretic mobilities are closed to (1*S*,2*S*)-PE, indicating closed three peaks at 20 to 25 mM DM-β-CD and co-migration of these three analytes at 50 mM DM-β-CD. This is in good agreement with the observed electropherograms in Figures 3.2d-f. For the predicted μ in Figure 3.3b, the suitable DM-β-CD concentrations of 10 to 20 mM are seen for simultaneous separation of AP, MA, PE, EP and NE enantiomers. At 10.0 mM DM-β-CD, (1*S*,2*R*)-EP, *S*-AP and *R*-AP have closed μ, indicating closed three peaks, while the values of Δμ for (1*R*,2*R*)-PE:(1*R*,2*S*)-EP and *S*-AP:*R*-AP are closed at 15.0 and 20.0 mM DM-β-CD, indicating closed peaks of each pair. The suitable DM-β-CD concentrations and the pattern of electropherograms are found to be in good agreement between prediction (Figure 3.3b) and experiment (Figures 3.2b-d).

It can be concluded from Section 3.1 that the optimum CD concentration for simultaneous separation of several pairs of enantiomers using single CD can be predicted from binding constants of enantiomers and CD concentration. The observed CD concentrations at maximum mobility difference and maximum resolution were in good agreement with theory, previously reported by Penn *et al.* [1993, 1994]. Over a wide range of CD concentrations, the excellent agreement was obtained between the observed and predicted values of the mobility difference. Using the equations for prediction of resolution for a pair of enantiomers, reported by Nhujak [2001], good agreement was obtained between the observed and predicted resolution over a wide range of CD concentrations. In addition, the observed value of maximum resolution was in good agreement with the simple equation $R_{s,max} = 30(\alpha-1)$, where α is the enantioselectivity, reported by Nhujak [2001]. Furthermore, the suitable CD concentration and the pattern of electropherogram for simultaneous separation of several pair of enantiomers can be predicted from plots of predicted μ and Δμ as a function of CD concentration.

3.2 Enantiomeric Separation Using Dual cyclodextrin

3.2.1 Principle of CE Chiral Separation Using Dual Cyclodextrins

In the presence of two types of cyclodextrins (CD1 and CD2) in the BGE, binding equilibria for enantiomers (*R* and *S*) are represented by

$$R + CD1 \underset{}{\overset{K_{1R}}{\rightleftharpoons}} RCD1 \qquad S + CD1 \underset{}{\overset{K_{1S}}{\rightleftharpoons}} SCD1$$

$$R + CD2 \underset{}{\overset{K_{2R}}{\rightleftharpoons}} RCD2 \qquad S + CD2 \underset{}{\overset{K_{2S}}{\rightleftharpoons}} SCD2$$

Equations defining the binding constants, *K*, are

$$K_{1R} = \frac{[RCD1]}{[CD1][R]} \qquad K_{1S} = \frac{[SCD1]}{[CD1][S]} \tag{3.14}$$

$$K_{2R} = \frac{[RCD2]}{[CD2][R]} \qquad K_{2S} = \frac{[SCD2]}{[CD2][S]} \tag{3.15}$$

From Equations 1.32, 1.33, 3.14 and 3.15, it follows that the electrophoretic mobilities of a pair of enantiomers are given by the equations, [Peng *et al.* 1997]

$$\mu_R = \frac{\mu_0 + K_{1R}C_1\mu_{\infty 1} + K_{2R}C_2\mu_{\infty 2}}{1 + K_{1R}C_1 + K_{2R}C_2} \tag{3.16}$$

$$\mu_S = \frac{\mu_0 + K_{1S}C_1\mu_{\infty 1} + K_{2S}C_2\mu_{\infty 2}}{1 + K_{1S}C_1 + K_{2S}C_2} \tag{3.17}$$

According to Equations 1.34, 3.16 and 3.17 for $K_R > K_S$, $\Delta\mu$ of enantiomers (μ_S-μ_R) in the dual CDs system can be expressed by the equation

$$\Delta\mu = \frac{\Delta K_1(\mu_o - \mu_{\infty 1})C_1 + \Delta K_2(\mu_o - \mu_{\infty 2})C_2 + (K_{2R}K_{1S} - K_{1R}K_{2S})\Delta\mu_\infty C_1C_2}{(1 + K_{1R}C_1 + K_{2R}C_2)(1 + K_{1S}C_1 + K_{1S}C_2)} \tag{3.18}$$

where $\Delta K_1 = K_{1R} - K_{1S}$ and $\Delta K_2 = K_{2R} - K_{2S}$

3.2.2 Theoretical Models of Mobility Difference

$\Delta\mu$ in Equation 3.18 may be rearranged to relate to $\bar{K}C$ and α as the equation

$$\Delta\mu = \frac{2\left(\frac{\alpha_1 - 1}{\alpha_1 + 1}\right)\bar{K}_1 C_1(\mu_o - \mu_{\infty 1}) + 2\left(\frac{\alpha_2 - 1}{\alpha_2 + 1}\right)\bar{K}_2 C_2(\mu_o - \mu_{\infty 2}) + 4\left(\frac{\alpha_2 - \alpha_1}{(\alpha_1 + 1)(\alpha_2 + 1)}\right)\bar{K}_1 C_1 \bar{K}_2 C_2(\mu_{\infty 1} - \mu_{\infty 2})}{(1 + \bar{K}_1 C_1 + \bar{K}_2 C_2)^2} \quad (3.19)$$

In order to describe and predict enantiomeric separation in the dual CDs system, theoretical models for $\Delta\mu$ of enantiomers in Equation 3.19 are firstly proposed in this work, and classified into five types based on enantioselectivity ratio ($\alpha_\alpha = \alpha_2/\alpha_1$).

Type I: $\alpha_\alpha > 1.0$, where $\alpha_2 > \alpha_1 \geq 1.0$

Type II: $\alpha_\alpha < 1.0$, where $\alpha_1 > \alpha_2 \geq 1.0$

Type III: $\alpha_\alpha = 1.0$, where $\alpha_2 = \alpha_1 > 1.0$

Type IV: $\alpha_\alpha < 1.0$, where $\alpha_1 \geq 1.0 \geq \alpha_2$

or $\alpha_\alpha > 1.0$, where $\alpha_2 \geq 1.0 \geq \alpha_1$

Type V: $\alpha_\alpha = 1.0$, where $\alpha_2 = \alpha_1 = 1.0$

Typically, the value of enantioselectivity is greater than 1.0. In the case of Types I, II and III where α_1 and $\alpha_2 > 1.0$, enantiomers have same migration order in the presence of single CD1 and CD2 in the BGE. In the case of Type IV, enantioselectivity less than 1.0 refers to the reversed migrating order for enantiomers using CD1 and CD2. Type V, where α_1 and α_2 are equal to 1.0, indicates co-migration of enantiomers and therefore,n no enantiomeric resolution is obtained using either single or dual CDs. In order to simply predict the values of $\Delta\mu$ for enantiomers at a fixed C_1 over a wide range of C_2, the values of $\mu_{\infty 1}$ and $\mu_{\infty 2}$ in Equation 3.19 are assumed to be identical, and therefore, $\Delta\mu$ in Equation 3.19 is given by the following simple equation

$$\Delta\mu = \frac{2\left(\left(\frac{\alpha_1 - 1}{\alpha_1 + 1}\right)\bar{K}_1 C_1 + \left(\frac{\alpha_2 - 1}{\alpha_2 + 1}\right)\bar{K}_2 C_2\right)}{(1 + \bar{K}_1 C_1 + \bar{K}_2 C_2)^2}(\mu_o - \mu_\infty) \quad (3.20)$$

From Equation 3.20, by keeping a constant C_1 in the BGE, the change of $\Delta\mu$ depends only on C_2 of CD2 added in the BGE. The CD2 concentration at maximum mobility difference, $C_{2,\Delta\mu_{max}}$ can be determined from Equation 3.20 by using differential calculus. When $d\Delta\mu/d\,\bar{K}_2C_2 = 0$

$$\bar{K}_2C_{2,\Delta\mu_{max}} = 1 + m\bar{K}_1C_1 \tag{3.21}$$

where

$$m = \left(1 - 2\frac{(\alpha_1 - 1)}{(\alpha_2 - 1)}\frac{(\alpha_2 + 1)}{(\alpha_1 + 1)}\right) \tag{3.22}$$

The values of α and $\bar{K}$ in Equation 3.20 are assumed as shown in Table 3.5, and μ_o-μ_∞ = 1.5 unit. Figure 3.9 shows two and three dimensional (2D and 3D) plots of the $\Delta\mu$ models of Type I to IV, using data in Table 3.5. At a fixed $\bar{K}_1C_1$ over a wide range of C_2. $\bar{K}_1C_1$ = 1 refers to the CD1 concentration giving maximum $\Delta\mu$. At $\bar{K}_1C_1$ = 0 or single CD in the BGE, a change of $\Delta\mu$ as a function of CD_2 is previously discussed in Section 3.1.3 and Figure 3.4.

Table 3.5 The assumed values of α and $\bar{K}$ used in theoretical models for $\Delta\mu$

Type	α			$\bar{K}_2$ (M^{-1})
	α_1	α_2	α_α	
I	1.05	1.20	1.14	100
II	1.20	1.05	0.88	100
III	1.20	1.20	1.00	100
IV	1.20	0.80	0.67	100

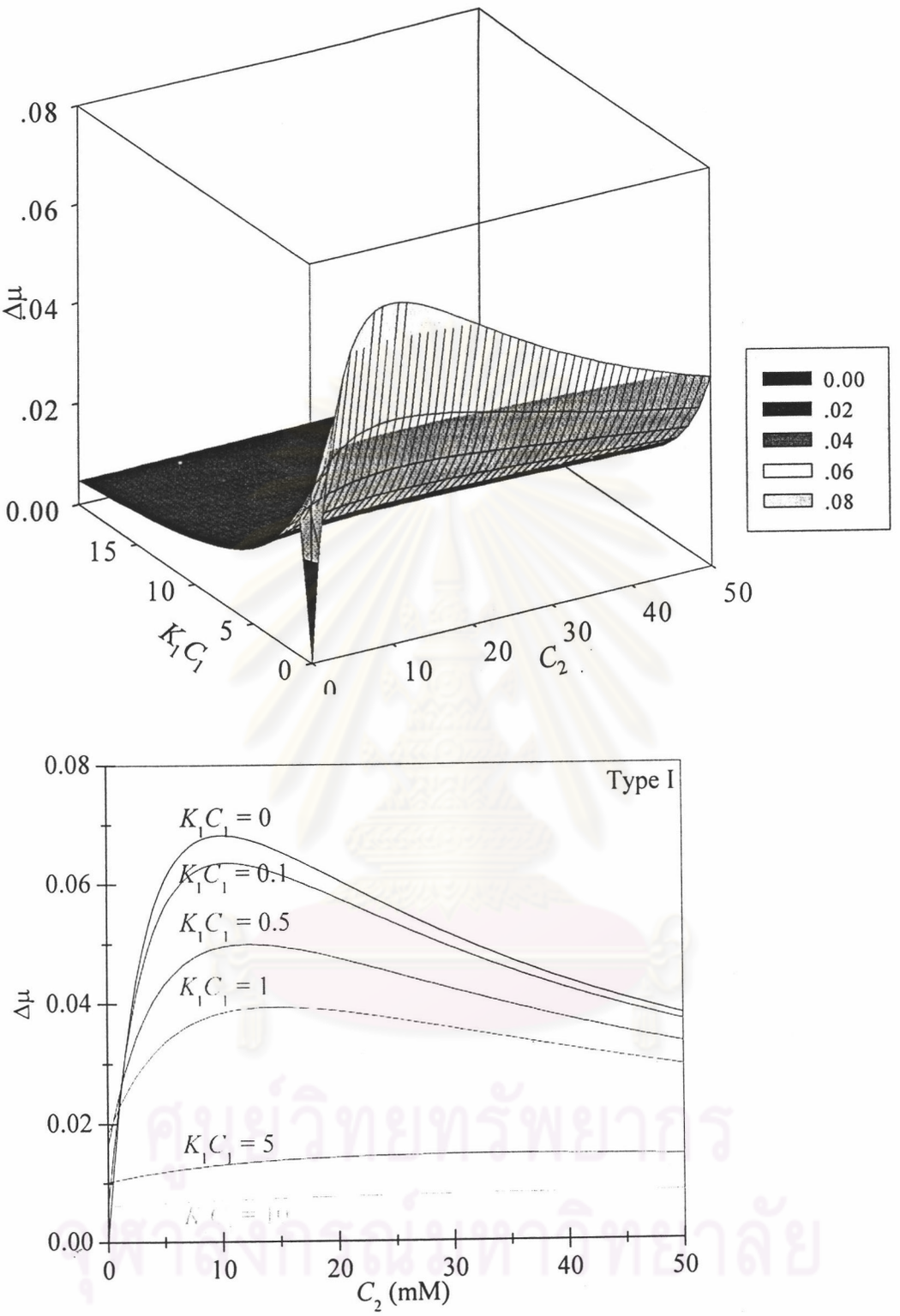

Figure 3.9a Theoretical models of Δμ of enantiomers in dual CDs system. Type I: $\alpha_\alpha > 1.0$, where $\alpha_2 > \alpha_1 \geq 1.0$. Δμ is obtained using Equation 3.20 and data in Table 3.5.

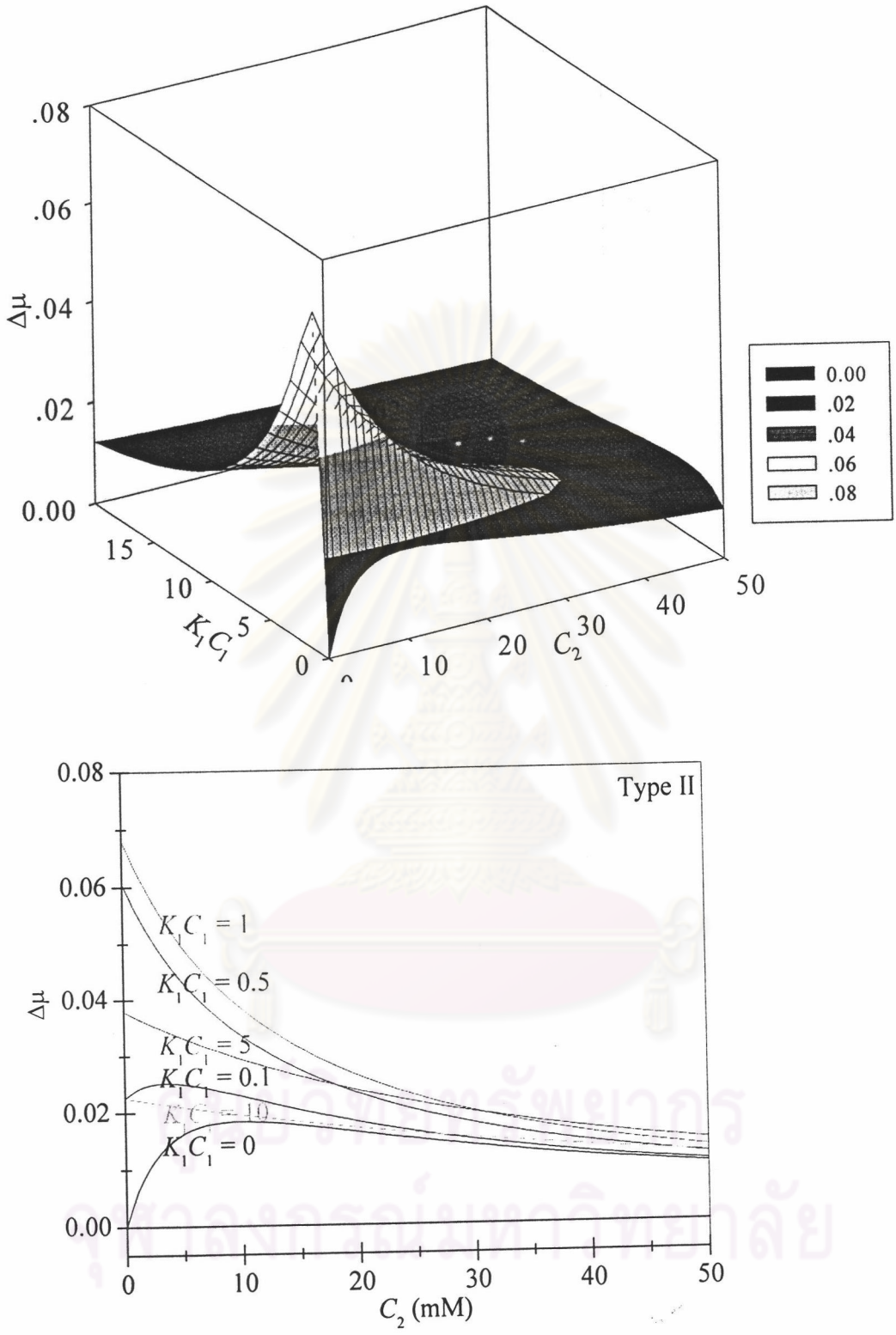

Figure 3.9b Continued. Type II: $\alpha_\alpha < 1.0$, where $\alpha_1 > \alpha_2 \geq 1.0$.

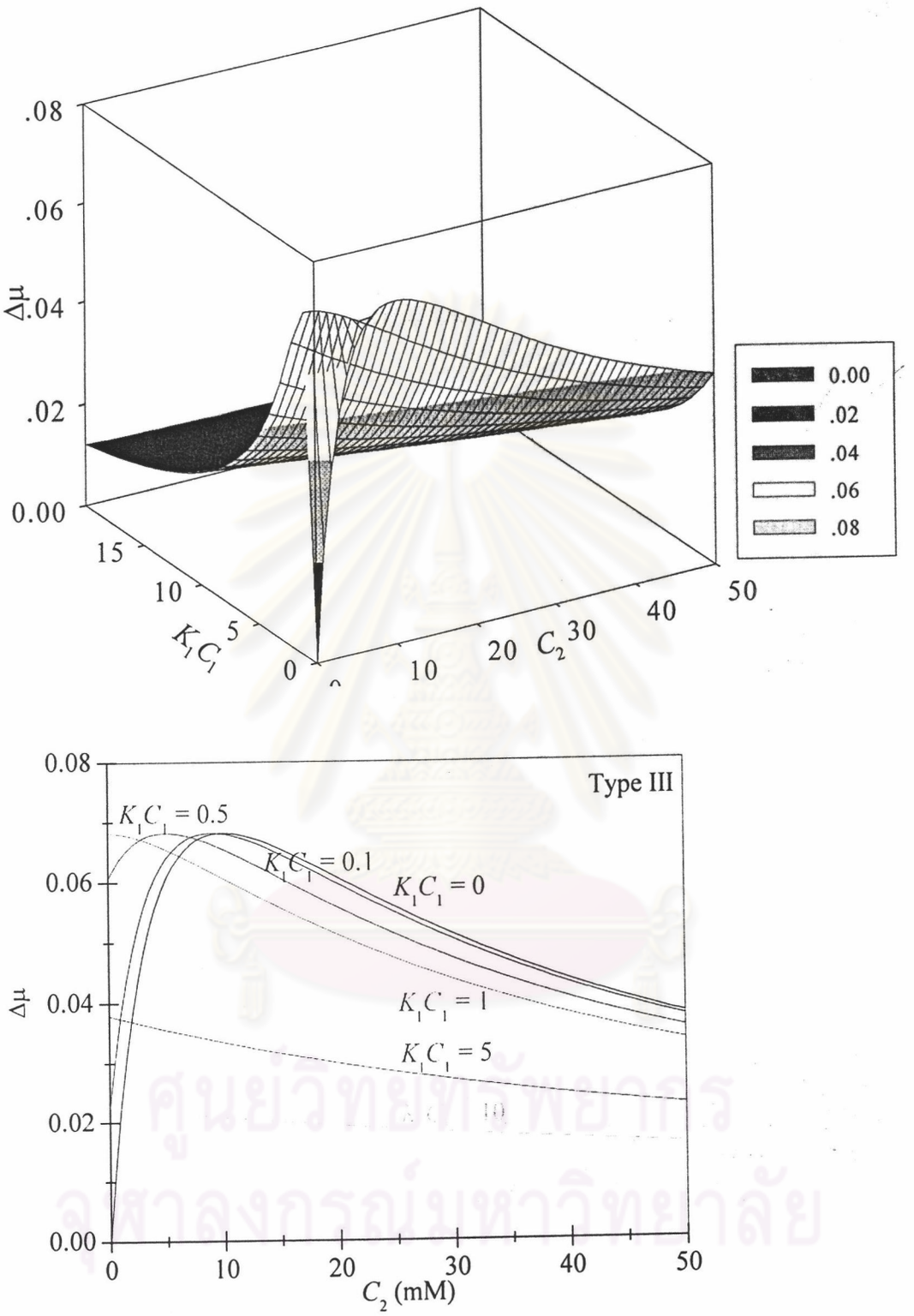

Figure 3.9c Continued. Type III: $\alpha_\alpha = 1.0$, where $\alpha_2 = \alpha_1 > 1.0$.

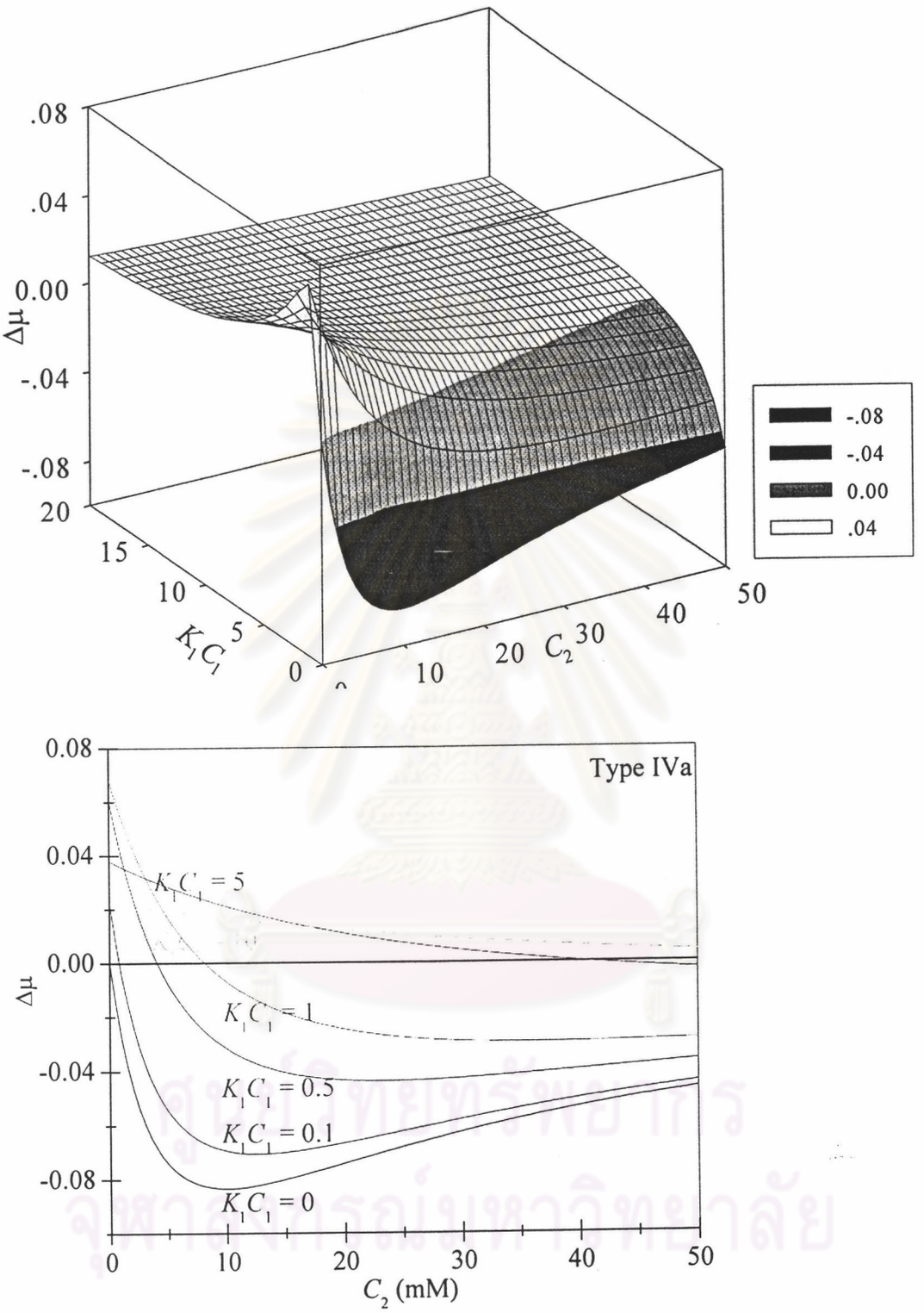

Figure 3.9d Continued. Type IVa: $\alpha_\alpha < 1.0$, where $\alpha_1 \geq 1.0 \geq \alpha_2$.

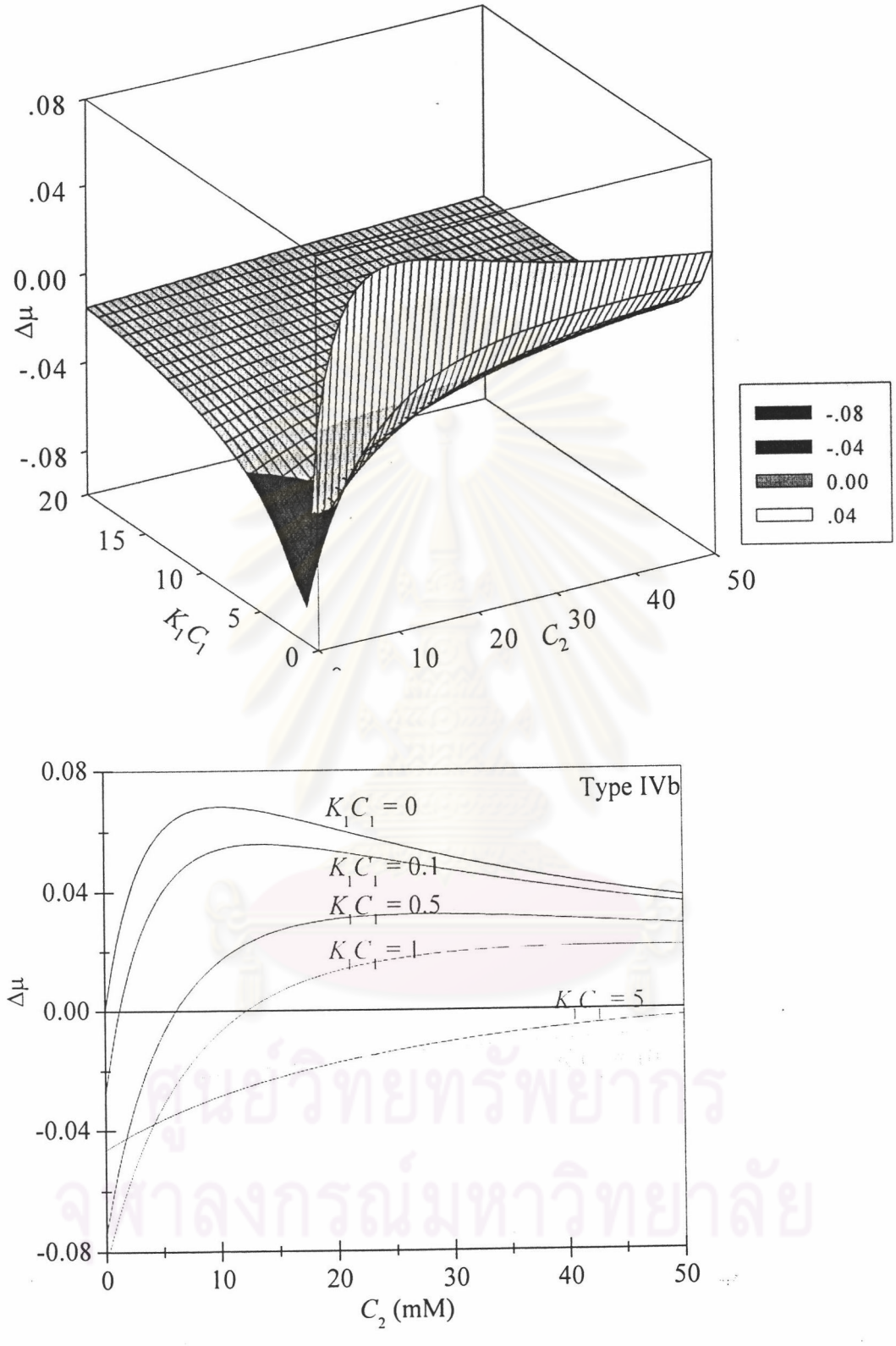

Figure 3.9e Continued. Type IVb: $\alpha_\alpha > 1.0$, where $\alpha_2 \geq 1.0 \geq \alpha_1$.

Figure 3.9a is firstly considered. At fixed CD1 concentration, for example, $\bar{K}_1C_1$ = 0.5 and 1.0 and 5.0, respectively, the values of Δμ as a function of CD_2 have the same trend, but the smaller the value of $\bar{K}_1C_1$, the higher the value of Δμ. In addition, the CD2 concentration giving $\Delta\mu_{max}$ increases with decreasing the fixed value of $\bar{K}_1C_1$. From Equation 3.21, when $\alpha_1 \approx 1$, the value of $m \approx 1$, giving the equation $\bar{K}_2C_{2,\Delta\mu_{max}} \approx 1+\bar{K}_1C_1$. Therefore, $C_{2,\Delta\mu_{max}}$ for dual CD system is higher than $C_{2,\Delta\mu_{max}}$ at single CD1 system. It can be concluded that if higher enantioselectivity for CD2 than that for CD1, addition of CD2 in the BGE containing CD1 results in an improvement of Δμ for enantiomers up to maximum depending on CD1 concentration, and reduction of Δμ at $\bar{K}_2C_2 > 1$.

Secondly, Type II in Figure 3.9b is considered. At fixed $\bar{K}_1C_1$ giving Δμ greater than Δμ at $\bar{K}_2C_2$ = 1 and $\bar{K}_1C_1$ = 0 (Δμ = 0.2 at C_2 = 10 mM), addition of CD2 in the BGE containing CD1 leads to a decrease of Δμ. In comparison with other values of $\bar{K}_1C_1$, CD1 concentration at $\bar{K}_1C_1$ = 1 gives the highest Δμ over a wide range of CD1 concentrations. From Equation 3.22 and data in Table 3.5 (α_1 = 1.20 and α_2 = 1.05 for Type II), the value of parameter m is equal to –6.45, giving $\bar{K}_2C_{2,\Delta\mu_{max}} = 1-6.45\bar{K}_1C_1$, Therefore, at $\bar{K}_1C_1$ > 0.16 (1/6.45), $C_{2,\Delta\mu_{max}}$ is not observed due to $C_{2,\Delta\mu_{max}} < 0$, indicating that CD1 without CD2 provides better Δμ. It can be summarized that CD2 with smaller enantioselectivity than CD1 gives worse Δμ, except for $\bar{K}_1C_1 < 1/m$.

Thirdly, consideration of Type III in Figure 3.9c is discussed. It is seen that, at high $\bar{K}_1C_1$, for example $\bar{K}_1C_1$ = 5, Δμ decreases with increasing C_2, while at low $\bar{K}_1C_1$, for example $\bar{K}_1C_1$ = 0.5, addition of a small amount of C_2 increases Δμ up to maximum with $C_{2,\Delta\mu_{max}}$ less than $C_{2,\Delta\mu_{max}}$ at C_1 = 0. This may be explained from Equations 3.21 and 3.22 that m = -1 for $\alpha_2 = \alpha_1$, giving $\bar{K}_2C_{2,\Delta\mu_{max}} = 1-\bar{K}_1C_1$. Therefore, maximum Δμ is observed, when $\bar{K}_1C_1 < 1$. For example at $\bar{K}_1C_1$ = 0.5, $C_{2,\Delta\mu_{max}}$ = 5, observed from Figure 3.9c and calculated using Equation 3.22 and $\bar{K}_2$=100. It can be concluded that, for dual

cyclodextrins with a similar enantioselectivity, the improvement of Δμ is obtained only when $\bar{K}_1C_1 + \bar{K}_2C_2 < 1$ and $C_2 < C_{2,\Delta\mu_{max}}$ at $\bar{K}_1C_1 = 1$.

Finally, the Δμ model for Type IVa in Figure 3.9d shows that, at fixed $\bar{K}_1C_1$, an increase in C_2 results in a decrease in Δμ to zero and then Δμ < 0. This indicateds tha reversed migration order of enantiomers in CD2 and CD1. The Δμ model for Type IVa and IVb are similar, but opposite sign of Δμ.

3.2.3 Prediction of Δμ Models for Enantiomers Amphetamine Drugs

In the case of a dual CDs system carried out by addition of DM-β-CD into the BGE containing β-CD, CD1 and CD2 refer to β-CD and DM-β-CD, respectively. On the other hand, in the case of a dual CDs system carried out by addition of β-CD into the BGE containing DM-β-CD, CD1 and CD2 refer to DM-β-CD and β-CD, respectively. For calculation of Δμ using Equation 3.19, values of parameters $\bar{K}$ and α obtained from Table 3.1 are summarized in Table 3.6, and values of parameters μ used are shown in Table 3.1.

Figure 3.10 shows 3D plots of predicted values of Δμ of enantiomers as a function of the concentration ($C_2 = C_{D\beta}$) of DM-β-CD added into the BGE containing β-CD at various values of $\bar{K}_\beta C_\beta$ ($\bar{K}_1C_1$), Figure 3.11 shows plots of predicted values of Δμ of enantiomers as a function of the concentration ($C_2 = C_\beta$) of β-CD added into the BGE containing DM-β-CD at various values of $\bar{K}_{D\beta}C_{D\beta}$ ($\bar{K}_1C_1$).

In comparison of Figures 3.10 and 3.11 with Figure 3.9, predicted models of Δμ of enantiomers in the dual CDs system are listed in Table 3.6. For the dual CDs system in Figure 3.10 where CD1 and CD2 are β-CD and DM-β-CD, respectively, models of Δμ for each pair of AP and MA enantiomers should be Type II due to $\alpha_\alpha < 1.0$ with α_β and $\alpha_{D\beta} \geq 1.0$, while Type I for PE and NE enantiomers due to $\alpha_\alpha > 1.0$ with α_β and $\alpha_{D\beta} \geq 1.0$. As previous results in Section 3.1.2, EP enantiomers have opposite migration order, using single CD as β-CD and DM-β-CD, therefore, Δμ of EP enantiomers are in agreement

with Type IVa due to $\alpha_\alpha < 1.0$ with $\alpha_\beta < 1.0 < \alpha_{D\beta}$. For the dual CDs system in Figure 3.11 where CD1 and CD2 are DM-β-CD and β-CD, respectively, the following models are classified for Δμ of enantiomers: AP and MA as Type I, PE and NE as Type II and EP as Type IVb.

Table 3.6 The values of $\bar{K}$ and α used in prediction of theoretical models for Δμ of test enantiomers

Addition of DM-β-CD (CD2) into the BGE containing β-CD (CD1)										
	CD		$\bar{K}$ (M^{-1})		α			Model of Δμ		
			$\bar{K}_1$	$\bar{K}_2$	α_1	α_2	α_α	Prediction	Experiment at C_β (mM)	
	1	2	$\bar{K}_\beta$	$\bar{K}_{D\beta}$	α_β	$\alpha_{D\beta}$			8.0	10.0
AP	β	DM-β	89.1	153.0	1.085	1.045	0.963	II	II	II
MA	β	DM-β	105.0	173.7	1.103	1.052	0.954	II	II	II
PE	β	DM-β	50.7	103.3	1.413	1.516	1.073	I	I	I
EP	β	DM-β	37.6	86.6	1.071	0.886	0.828	IVa	IVa	IVa
NE	β	DM-β	29.8	64.4	1.000	1.187	1.187	I	I	I
Addition of β-CD (CD2) into the BGE containing DM-β-CD (CD1)										
	CD		$\bar{K}$ (M^{-1})		α			Model of Δμ		
			$\bar{K}_1$	$\bar{K}_2$	α_1	α_2	α_α	Prediction	Experiment at $C_{D\beta}$ (mM)	
	1	2	$\bar{K}_{D\beta}$	$\bar{K}_\beta$	$\alpha_{D\beta}$	α_β			6.0	10.0
AP	DM-β	β	153.0	89.1	1.045	1.085	1.038	I	I	I
MA	DM-β	β	173.7	105.0	1.052	1.103	1.048	I	I	I
PE	DM-β	β	91.7	103.3	1.516	1.413	0.932	II	II	II
EP	DM-β	β	86.6	37.6	0.886	1.071	1.209	IVb	IVb	IVb
NE	DM-β	β	64.4	29.8	1.187	1.000	0.842	II	II	II

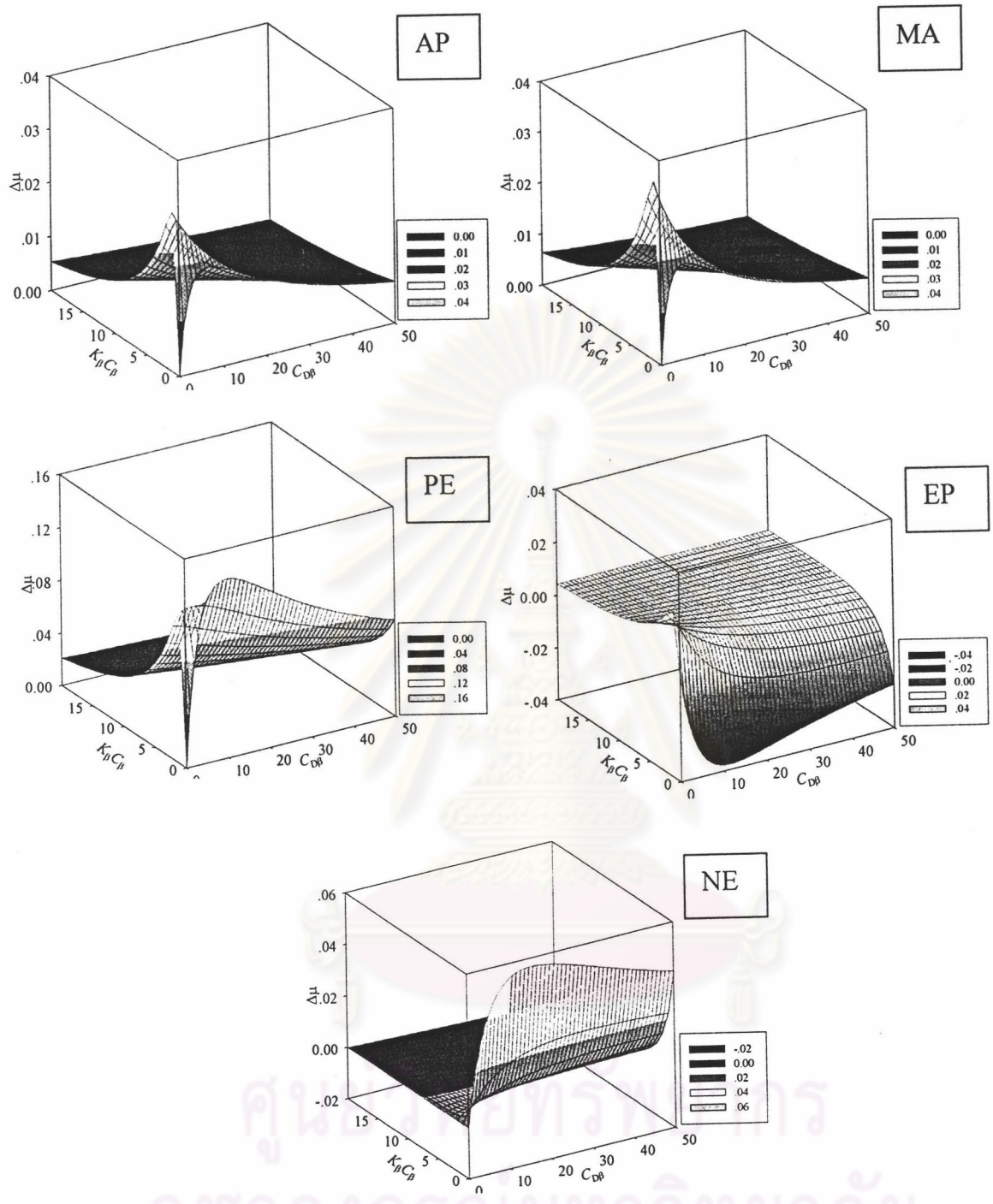

Figure 3.10 Theoretical models of Δμ of AP, MA, PE, EP and NE enantiomers in dual CDs system over a wide range of $C_{D\beta}$ at fixed C_β. Δμ is obtained from Equation 3.19 and data in Table 3.6.

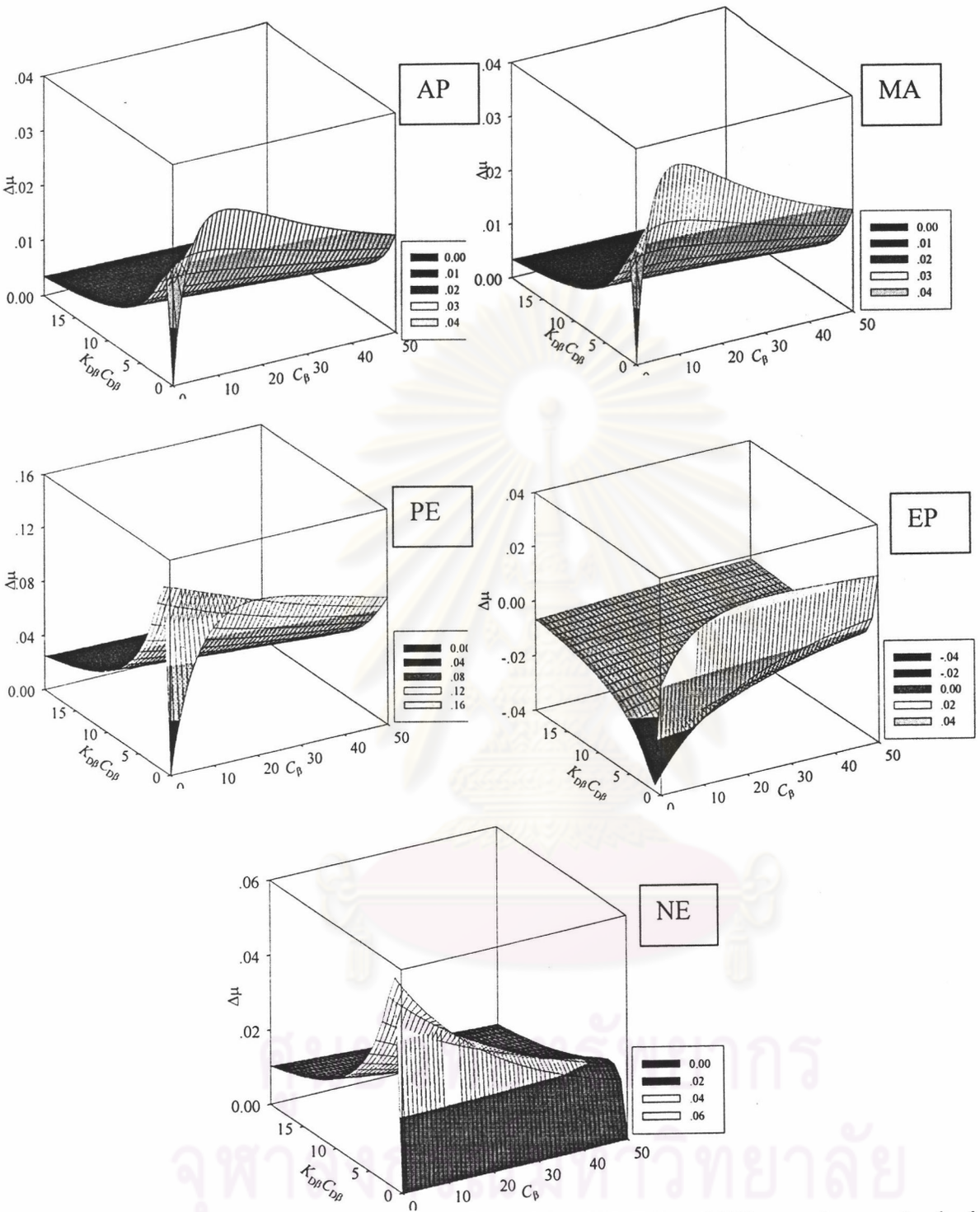

Figure 3.11 Theoretical models of Δμ of AP, MA, PE, EP and NE enantiomers in dual CDs system over a wide range of C_β at fixed $C_{D\beta}$. Δμ is obtained from Equation 3.19 and data in Table 3.6.

3.2.4 Experimental and Predicted Values of Δμ for Enantiomers in Dual CDs

Figures 3.12 and 3.13 show an example of electropherograms of simultaneous separation of test enantiomers in dual CDs using (i) a fixed β-CD concentration and various DM-β-CD concentrations and (ii) a fixed DM-β-CD concentration and various β-CD concentrations, respectively. Fixed concentration (C_1) of 10.0 mM β-CD or DM-β-CD was chosen because it gave suitable R_s for simultaneous separation of all test analytes in a single CD system. From theoretical models of Δμ in Sections 3.2.2 and 3.2.3, the high values of KC_1, especially greater than 1.0, result in the small value of Δμ for enantiomers in dual CDs. Therefore, fixed 8.0 mM β-CD and 6.0 mM DM-β-CD ($KC_1 < 1.0$) were also chosen for investigation of Δμ of enantiomers in the dual CDs systems.

Figure 3.14 shows experimental and predicted Δμ of enantiomers in dual CDs system over a wide range of $C_{D\beta}$ at fixed C_β of 6.0 and 10.0 mM, and Figure 3.15 shows experimental and predicted Δμ of enantiomers in dual CDs system over a wide range of β-CD at fixed $C_{D\beta}$ of 8.0 and 10.0 mM. Good agreement was obtained between observed and predicted Δμ of enantiomers. From Figure 3.14 at fixed 8.0 and 10.0 mM β-CD, experimental results and prediction show that values of Δμ for each pair of AP and MA enantiomers decrease with increasing $C_{D\beta}$, which is in agreement with prediction as Type II of the Δμ model as previously mentioned. Δμ for of EP enantiomers also decreases to zero, due to reversed migration order. This is consistent with to Type IVa of the Δμ model. As non-enantioselectivity of β-CD for NE ($\alpha_{\beta,NE} = 1.0$), without DM-β-CD in the BGE containing β-CD, no resolution of NE enantiomers was obtained. According to Type I of the Δμ model, increasing DM-β-CD from 0 up to 30.0 mM resulted in an increase in Δμ of PE ($\alpha_\alpha = 1.073$). and NE enantiomers ($\alpha_\alpha = 1.187$).

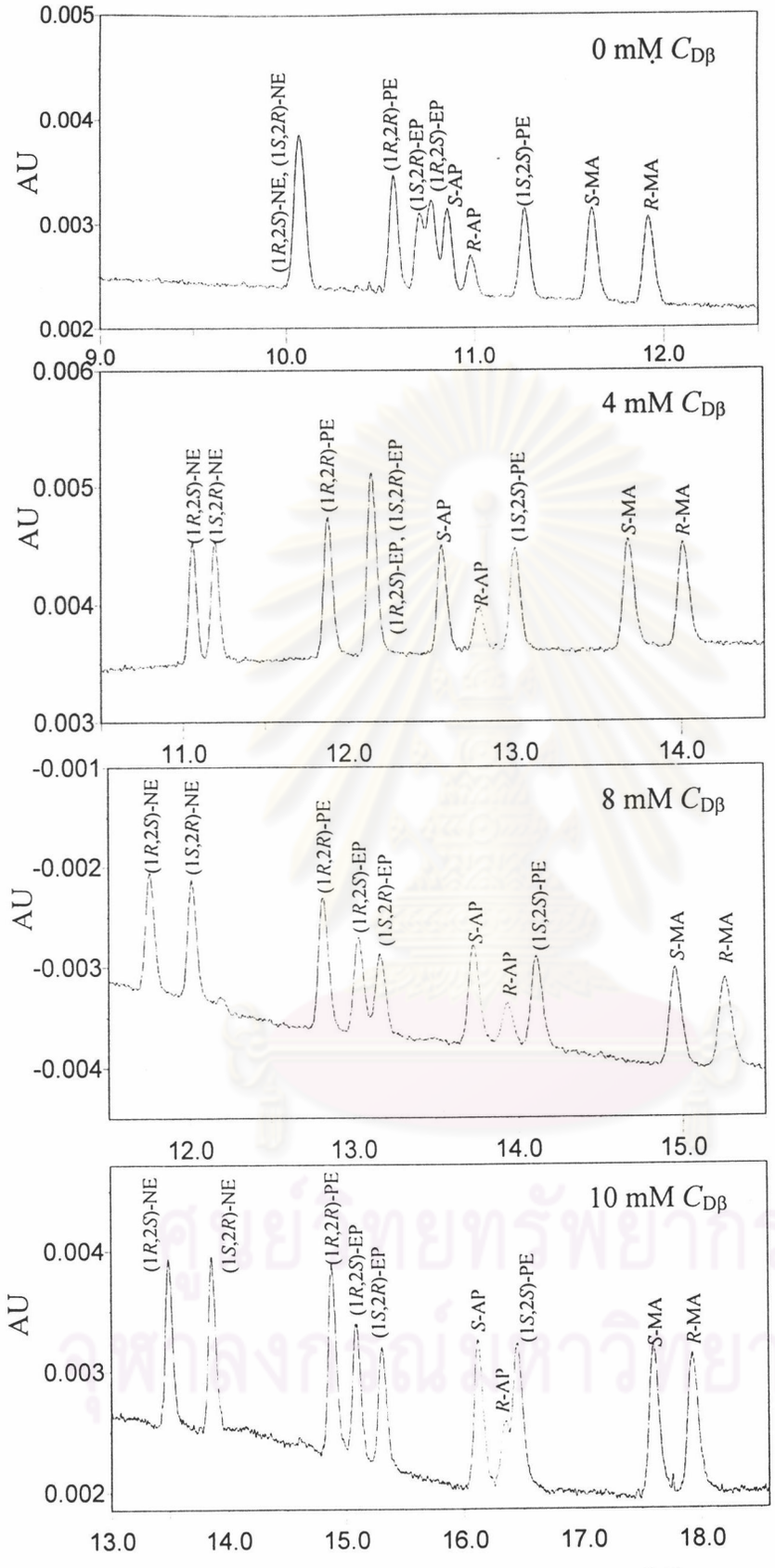

(a) fixed 8.0 mM C_{β} over a wide range of $C_{D\beta}$

Figure 3.12 Electropherograms of enantiomeric separation of AP, MA, PE, EP and NE using dual CDs as chiral selectors at fixed (a) 8.0 and (b) 10.0 mM C_{β} and various $C_{D\beta}$. CE conditions as shown in Figure 3.1.

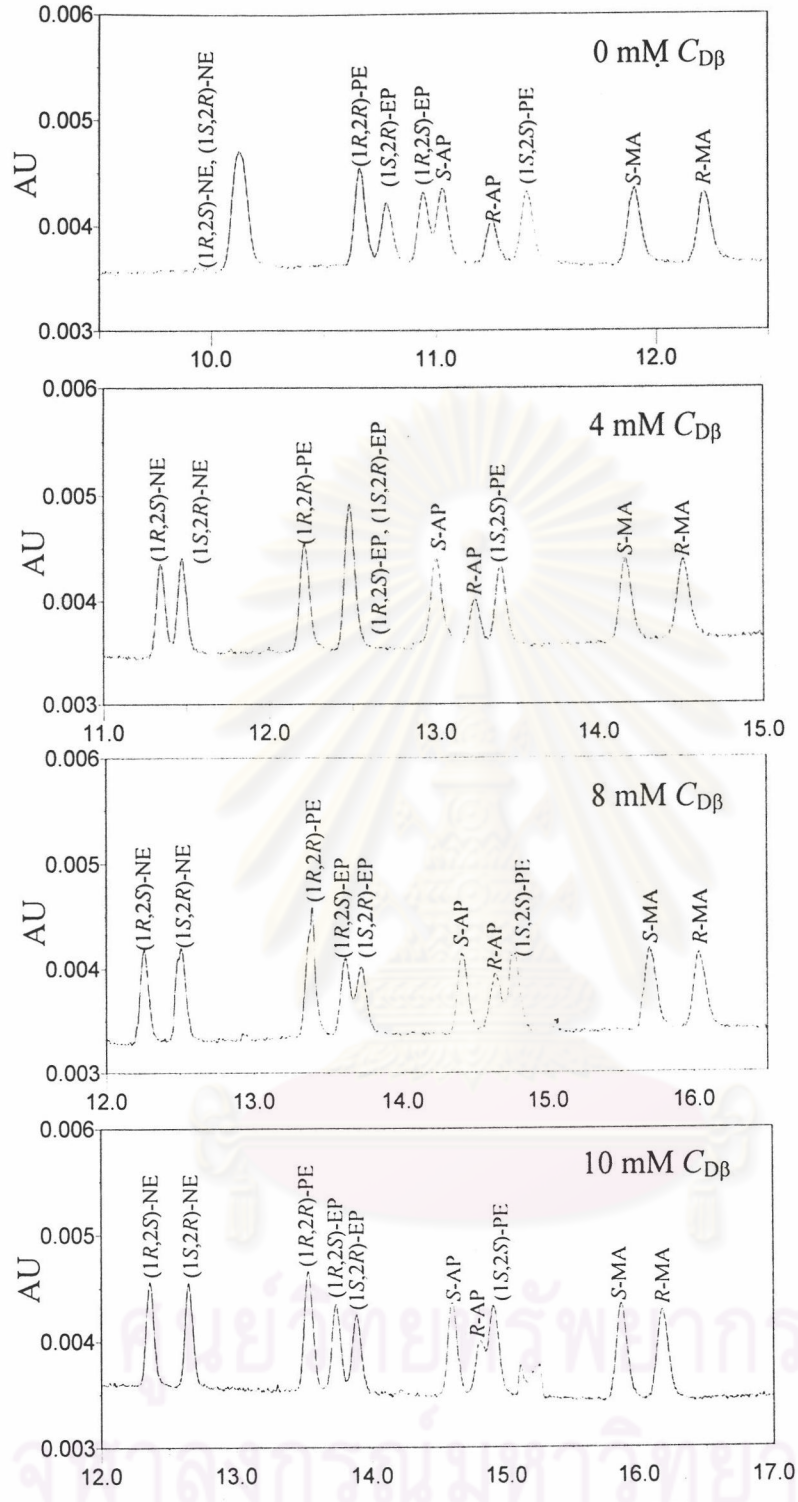

(b) fixed 10.0 mM C_{β} over a wide range of $C_{D\beta}$

Figure 3.12 Continued.

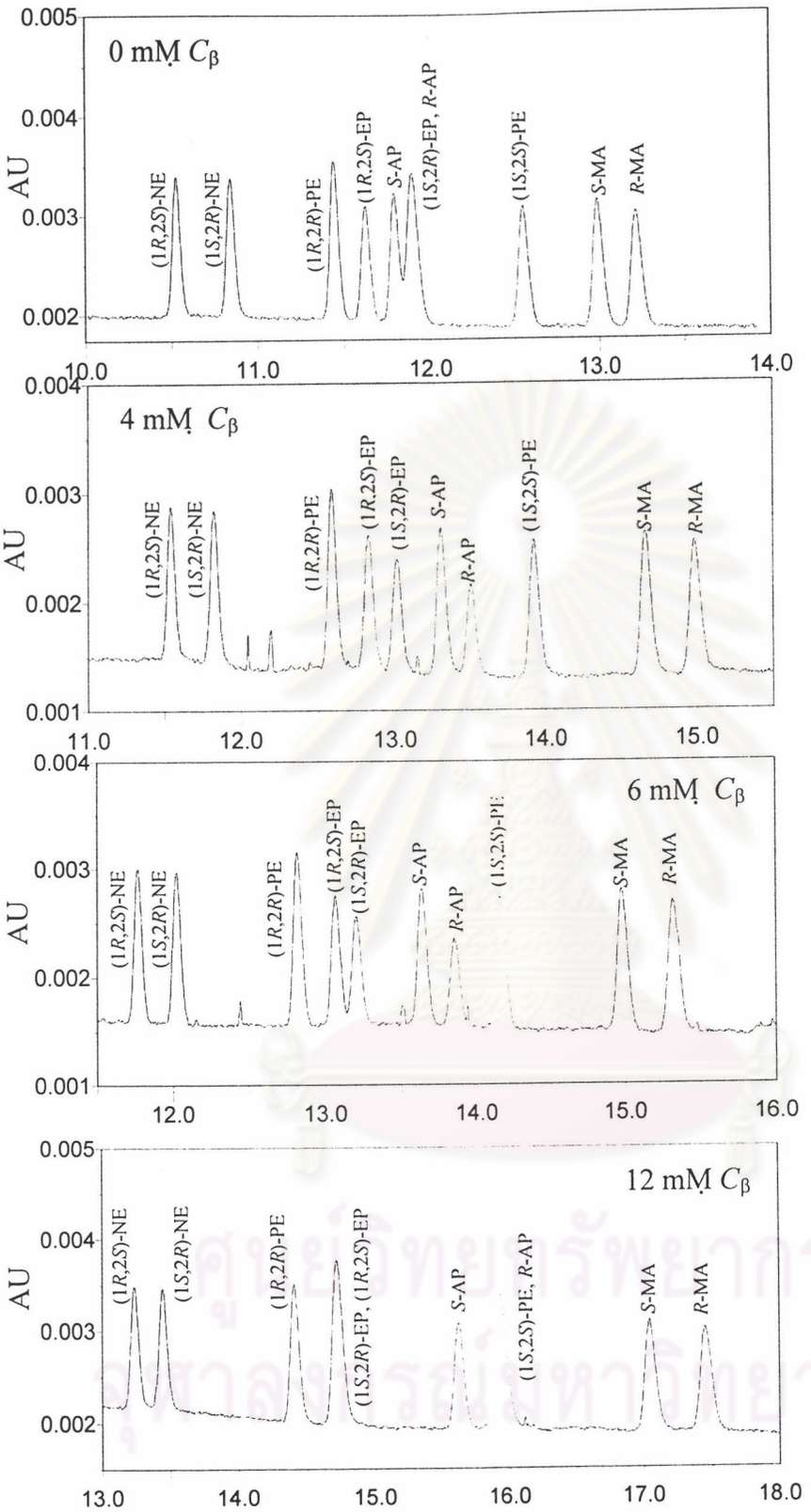

(a) fixed 6.0 mM $C_{D\beta}$ over a wide range of C_β

Figure 3.13 Electropherograms of enantiomeric separation of AP, MA, PE, EP and NE using dual CDs as chiral selectors at fixed (a) 6.0 and (b) 10.0 mM $C_{D\beta}$ and various C_β. CE conditions as shown in Figure 3.1.

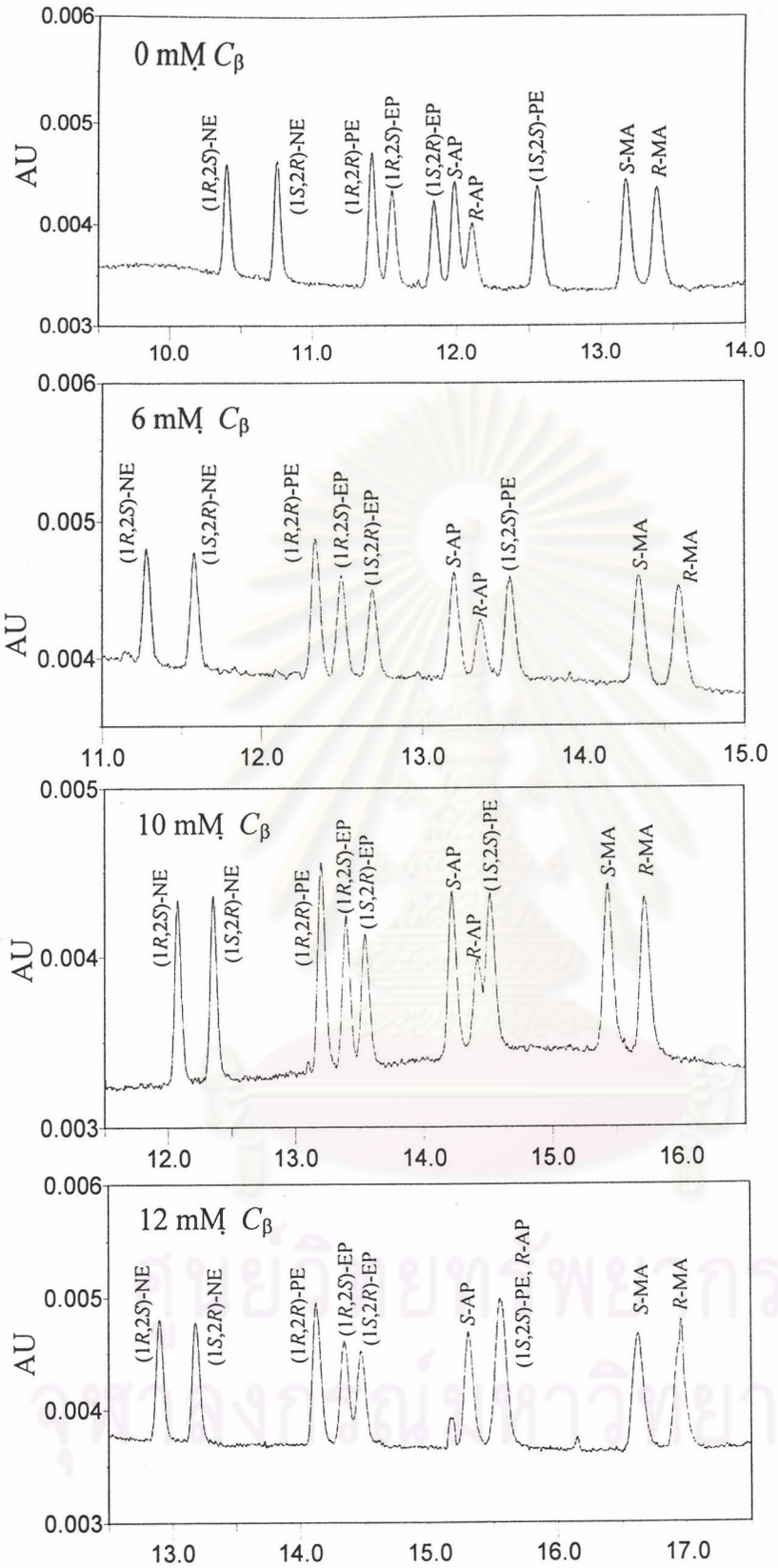

(b) fixed 10.0 mM $C_{D\beta}$ over a wide range of C_β

Figure 3.13 Continued.

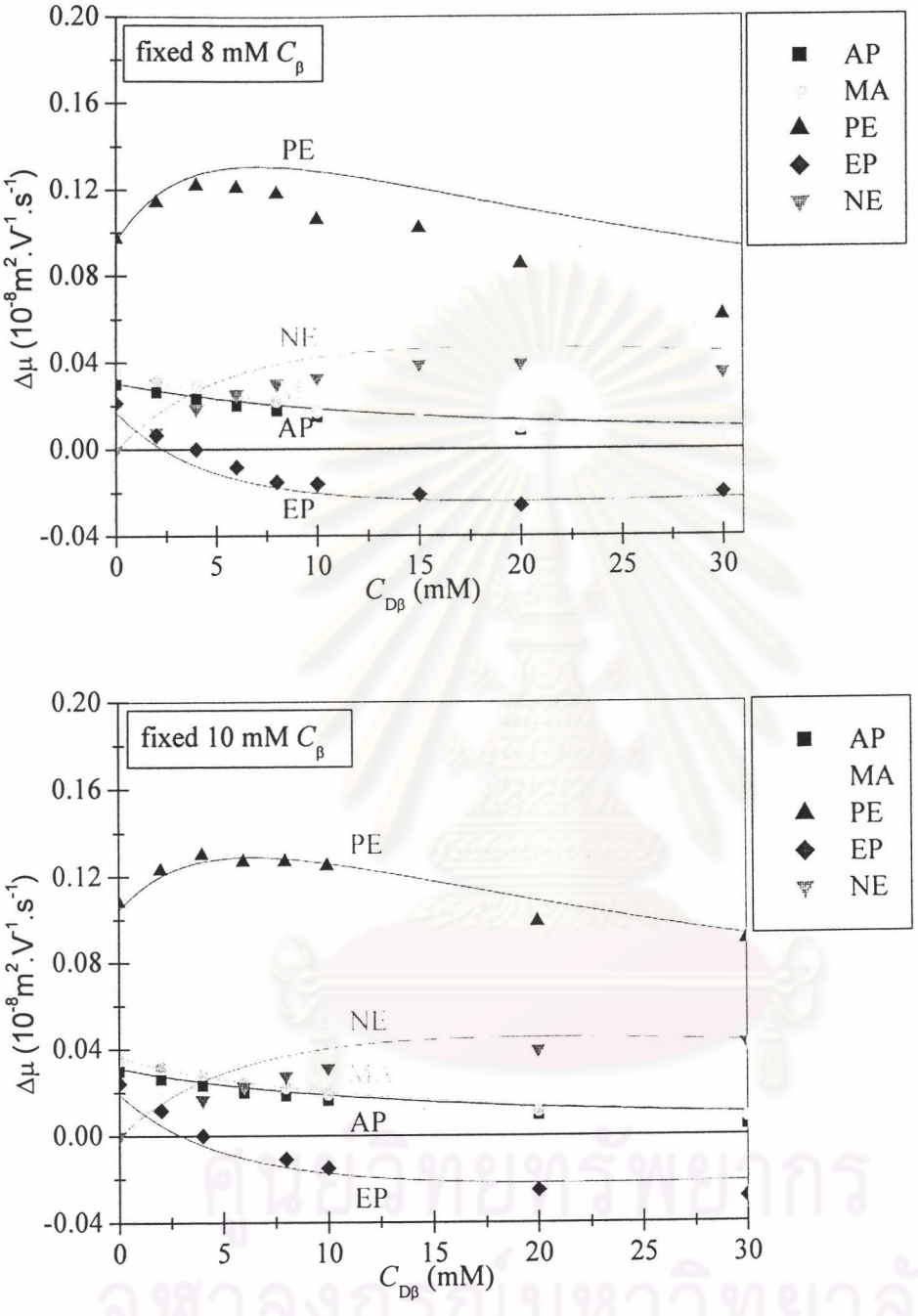

Figure 3.14 Observed (symbols) and predicted (solid lines) values of $\Delta\mu$ of enantiomers in dual CDs system over a wide range of $C_{D\beta}$ at fixed C_β of 8.0 and 10.0 mM. Predicted $\Delta\mu$ is obtained using Equation 3.19 and data in Tables 3.1 and 3.6.

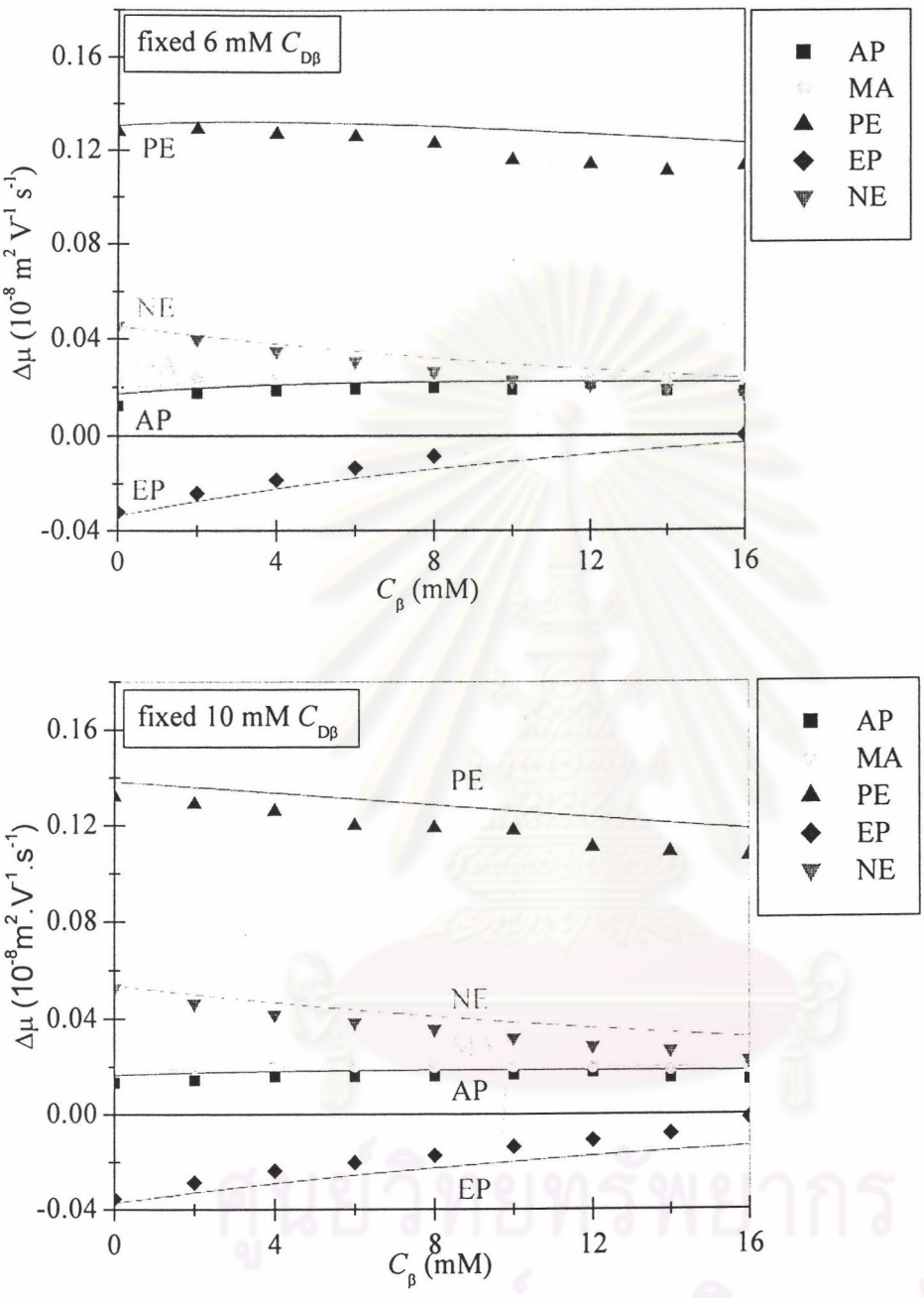

Figure 3.15 Observed (symbols) and predicted (solid lines) values of $\Delta\mu$ of enantiomers in dual CDs system over a wide range of C_β at fixed $C_{D\beta}$ of 6.0 and 10.0 mM. Predicted $\Delta\mu$ is obtained using Equation 3.19 and data in Tables 3.1 and 3.6.

From Figure 3.15, at fixed 6.0 and 10.0 mM DM-β-CD, experimental and predicted values of Δμ for each pair of AP and MA enantiomers slightly increase with increasing C_β in the range of 0 to 16.0 mM, which is consistent with Type I of the Δμ model. However, C_β giving maximum Δμ is higher than 16.0 mM and is not observed in this experiment because the solubility of β-CD in water is in the range of 0 to 16.0 mM as previously mentioned. Experimental and predicted values of $|\Delta\mu|$ for each pair of PE, EP and NE enantiomers decrease with increasing C_β over a wide range of 0 to 16.0 mM, which are in agreement with the Δμ model of Type IVb for EP ($\alpha_\alpha > 1$, $\alpha_{D\beta,EP} > 1 > \alpha_{\beta,EP}$) and Type II for PE and NE ($\alpha_\alpha < 1$, $\alpha_{D\beta} > \alpha_\beta \geq 1$).

It can be concluded that, over a wide range of CD2 at a fixed CD1 concentration, the values of experimental Δμ for AP, MA, PE, EP and NE enantiomers are found to be in agreement with the proposed Δμ models based on the enantioselectivity ratio of dual CDs for each pair of enantiomers. Enantiomeric separation using dual CDs may result in better or poorer Δμ of enantiomers, depending on the enantioselectivity ratio of dual CDs and the concentration of each CD used. At the fixed of C_β of 8.0 or 10.0 mM, addition of 0 to 30.0 mM DM-β-CD in the BGE containing β-CD resulted in poorer Δμ for AP and MA enantiomers, while provided better Δμ for PE and NE enantiomers. For EP enantiomers, worse Δμ was obtained when addition of 0 to 4 mM DM-β-CD, while Δμ improved when addition of DM-β-CD above 4 mM. For dual CDs system carried out by addition of β-CD in the BGE containing DM-β-CD, the values of Δμ for each pair PE, EP and NE enantiomers decreased with increasing C_β from 0 to 16.0 mM, while slightly increased of Δμ for each pair AP and MA enantiomers.

3.2.5 Peak Variance and Resolution in Dual CDs System

3.2.5.1 Predicted Peak Variance in Dual CDs System

Two major contributions, longitudinal diffusion and electromigration dispersion, were also taken into accounted for prediction of peak variance in the dual CDs system, similar to the single CD system as previously discussed in Section 3.1.4.1. In the dual CDs system, equations involving peak variance as a function *KC* of dimentionless were first derived in this work and based on Equations 3.8 and 3.10. From Equations 1.16, 1.17, 1.33, 2.2 and 3.8 the values of σ^2_{diff} and σ^2_{EMD} may be calculated using the equations

$$\sigma^2_{diff} = \frac{2kTlL}{zeV}\left(\frac{\frac{\mu^o_{\infty 2}}{\mu^o_{\infty 1}}\left(\frac{\mu^o_o}{\mu^o_{\infty 2}} + K_2C_2\right) + K_1C_1}{\frac{\mu_{\infty 2}}{\mu_{\infty 1}}\left(\frac{\mu_o}{\mu_{\infty 2}} + K_2C_2\right) + K_1C_1}\right)\frac{\mu^o_{\infty 1}}{\mu_{\infty 1}} \qquad (3.23)$$

$$\sigma^2_{EMD} = \left|\frac{2}{9} ll_{inj} c_A a_A\right| \qquad (3.24)$$

where the value of μ_A/μ_C used for calculation of parameter a_A in Equations 1.21 and 3.11 is given by

$$\frac{\mu_A}{\mu_C} = \left(\frac{\frac{\mu_{\infty 2}}{\mu_{\infty 1}}\left(\frac{\mu_o}{\mu_{\infty 2}} + K_2C_2\right) + K_1C_1}{1 + K_1C_1 + K_2C_2}\right)\frac{\mu_{\infty 1}}{\mu_C} \qquad (3.25)$$

Other parameters are previously defined as in Equations 3.8 to 3.11. Figure 3.16. shows the average values of σ^2_{diff} and σ^2_{EMD} and σ^2_{tot} for each enantiomer, calculated using Equations 3.23 to 3.25, $\bar{K}C$ and data in Tables 3.1 and 3.3.

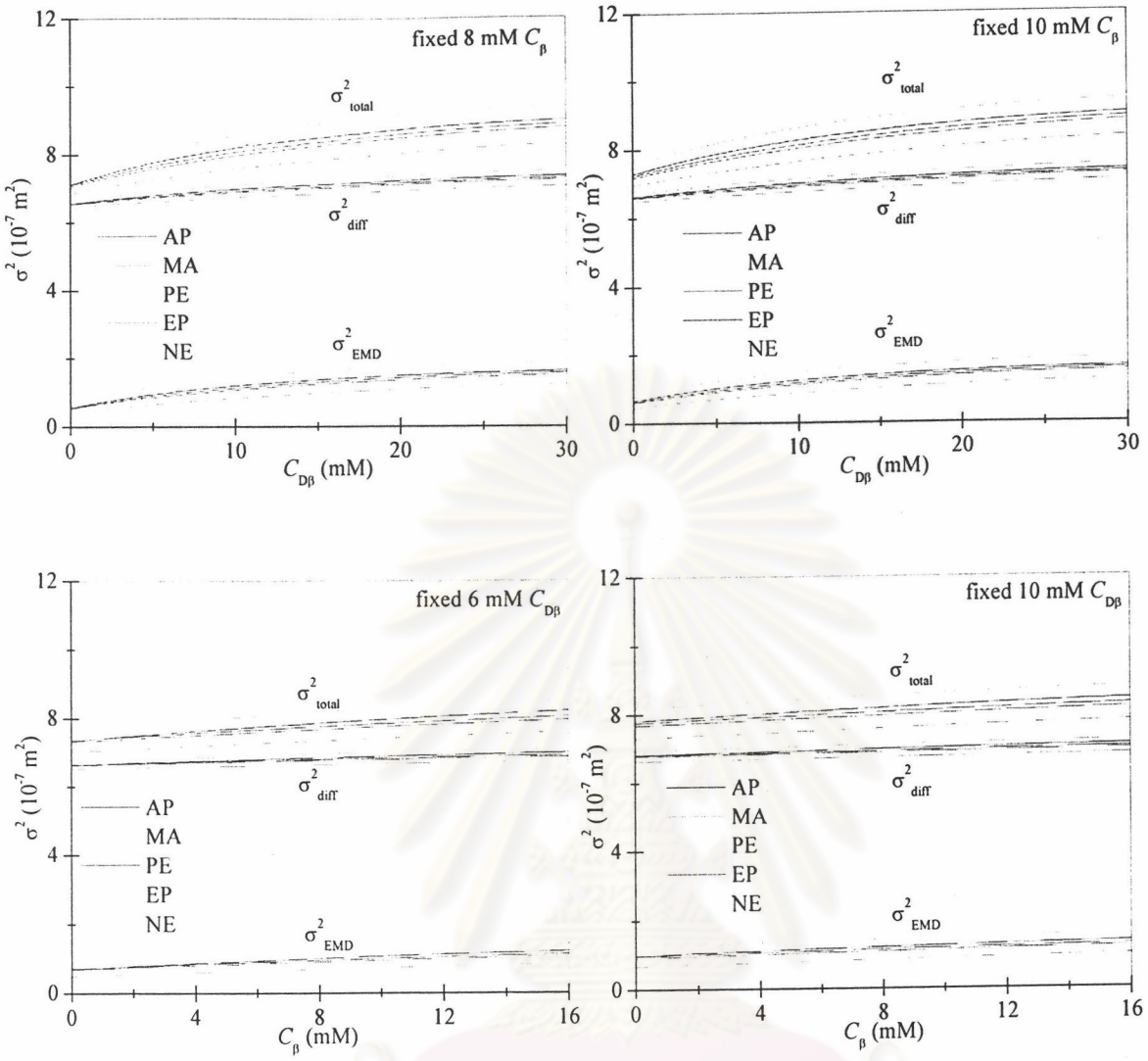

Figure 3.16 Predicted peak variance for AP, MA, PE, EP and NE enantiomers in dual cyclodextrins. σ^2 is the average for each pair of enantiomers. σ^2_{diff} and σ^2_{EMD} are obtained from Equations 3.23 and 3.24, respectively, and data from Tables 3.1 and 3.6.

3.2.5.2 Comparison of Observed and Predicted Total Peak Variance

Figures 3.17 and 3.18 show a comparison of observed and predicted values of σ^2_{tot} at fixed C_β over a wide range of $C_{D\beta}$ and fixed $C_{D\beta}$ over a wide range of C_β, respectively. Each predicted value (solid line) of σ^2_{tot} is the average for a pair of enantiomers as previously mentioned in Section 3.1.5.1. The observed value of σ^2_{tot} was obtained from measurement of peak width at base from electropherograms similar to the single CD system. Each observed value is for each isomer. Some observed σ^2_{tot} cannot be determined due to very closed peaks or co-migration. At fixed CD1 concentration and over a wide range of CD2 concentrations (Figures 3.17 and 3.18), the observed values σ^2_{tot} are approximately 10 to 100% higher than the predicted values. The result of this difference is due to other sources, especially analyte-wall absorption and extra EMD, similar to the single CD system as previously discussed in Section 3.1.4.2.

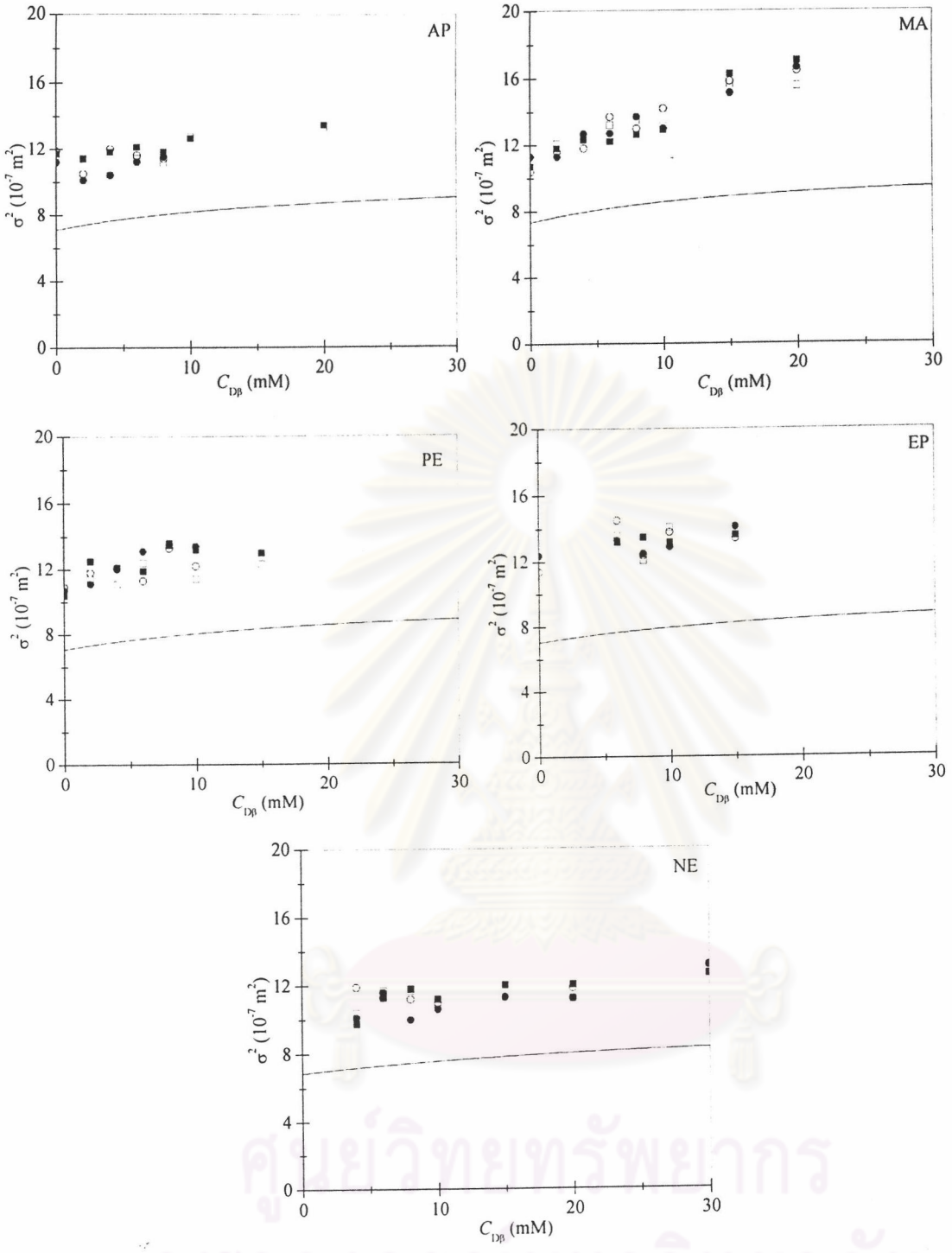

(a) fixed 8.0 mM C_β over a wide range of $C_{D\beta}$

Figure 3.17 Observed (symbols) and predicted (solid lines) values of total peak variance (σ^2_{tot}) for AP, MA, PE, EP and NE enantiomers using dual cyclodextrins at fixed (a) 8.0 and (b) 10.0 mM C_β with a wide range of $C_{D\beta}$. The predicted value is the average for each pair of enantiomers obtained from Figures 3.16a and 3.16b, respectively. The observed value is obtained from each isomer for each run. The black and blank symbols refer to the first and second run, respectively.

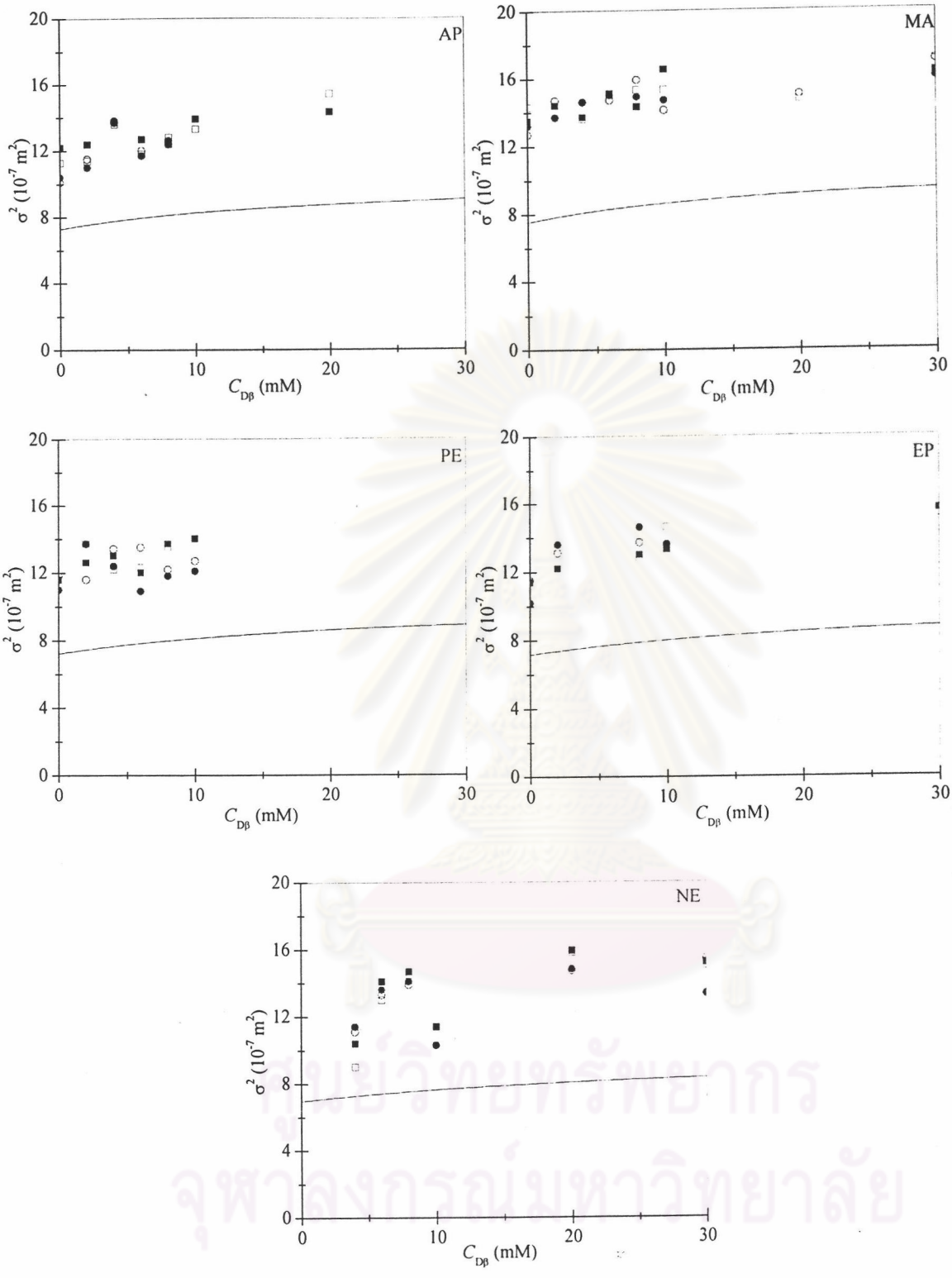

(b) fixed 10.0 mM C_β over a wide range of $C_{D\beta}$

Figure 3.17 Continued.

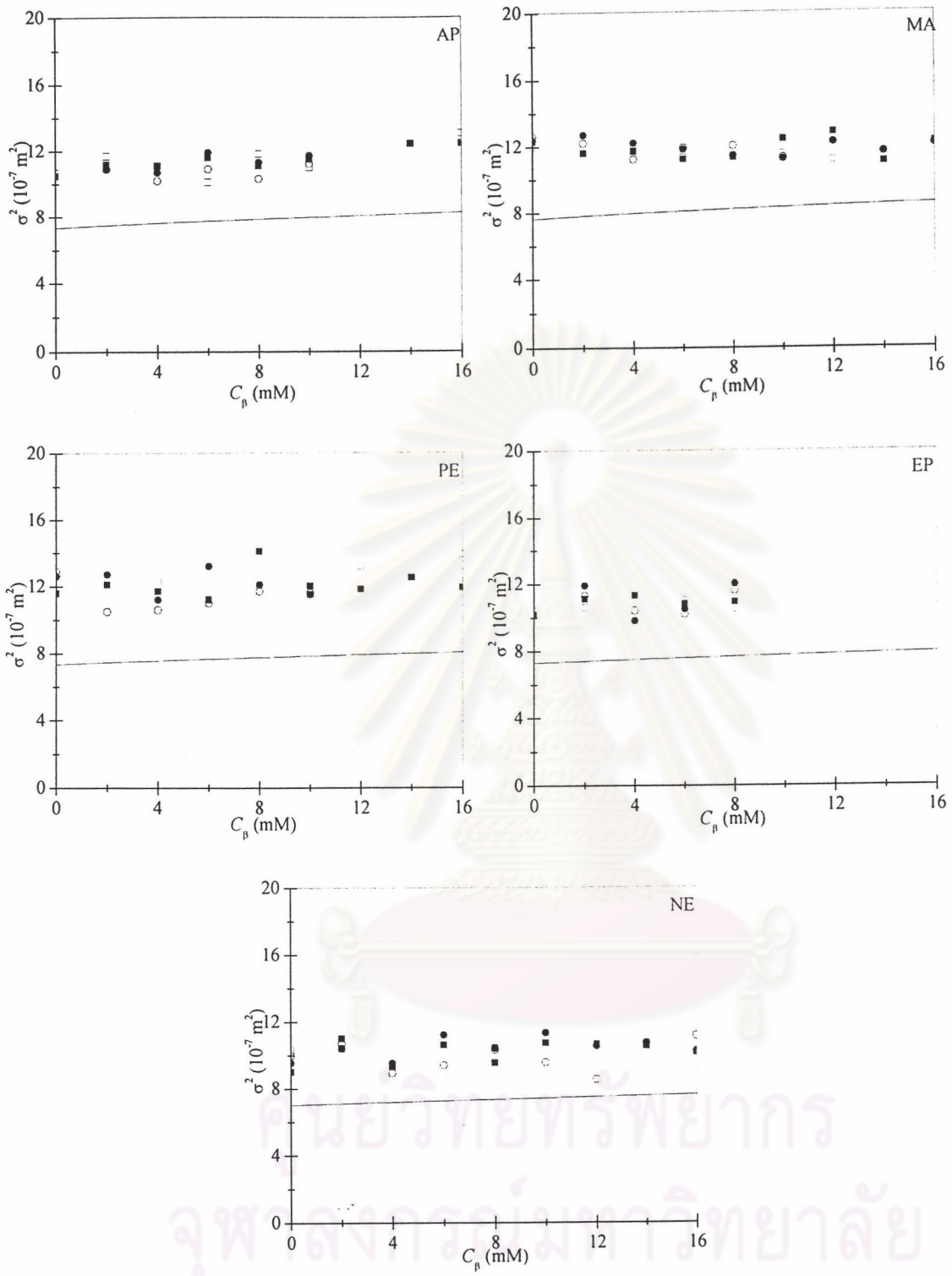

(a) fixed 6.0 mM $C_{D\beta}$ over a wide range of C_β

Figure 3.18 Observed (symbols) and predicted (solid lines) values of total peak variance (σ^2_{tot}) for AP, MA, PE, EP and NE enantiomers using dual cyclodextrins at fixed (a) 6.0 and (b) 10.0 mM $C_{D\beta}$ with a wide range of C_β. The predicted value is the average for each pair of enantiomers obtained from Figures 3.16c and 3.16d, respectively. The observed value is obtained from each isomer for each run. The black and blank symbols refer to the first and second run, respectively.

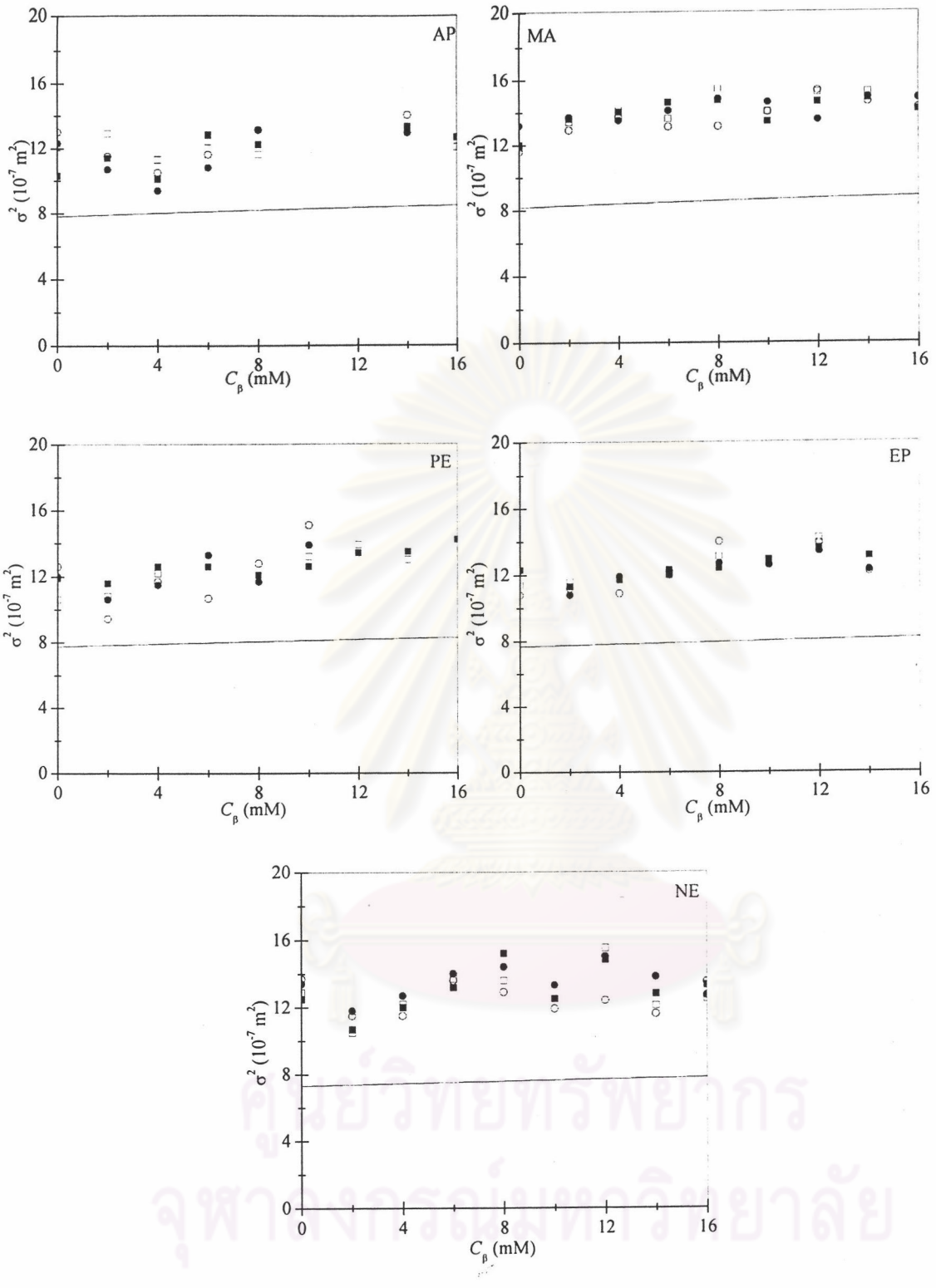

(b) fixed 10.0 mM $C_{D\beta}$ over a wide range of C_β

Figure 3.18 Continued.

3.2.5.3 Observed and Predicted Peak Efficiency

Figures 3.19 and 3.20 show a comparison of observed and predicted peak efficiency of each pair at fixed C_β over a wide range of $C_{D\beta}$ and fixed $C_{D\beta}$ over a wide range of C_β, respectively. The average value of peak efficiency (N) was calculated using Equation 1.12 and data in Figures 3.17 and 3.18, respectively. The observed $\bar{N}$ for each pair of enantiomers is obtained from the same run. At fixed CD1 concentration and over the wide range of CD2 concentrations, observed values of $\bar{N}$ were found to be in the range $\approx$ (1.5 to 2.5) $\times 10^5$, except for NE whose $\bar{N}$ of (2.2 to 3.0) $\times 10^5$ was observed at fixed 6.0 mM $C_{D\beta}$ over a wide range of C_β. With an increase in CD concentration, the predicted values of $\bar{N}$ decreased from 3.6×10^5 to 2.8×10^5. The observed $\bar{N}$ less than prediction is due to the observed σ^2_{tot} higher than prediction.

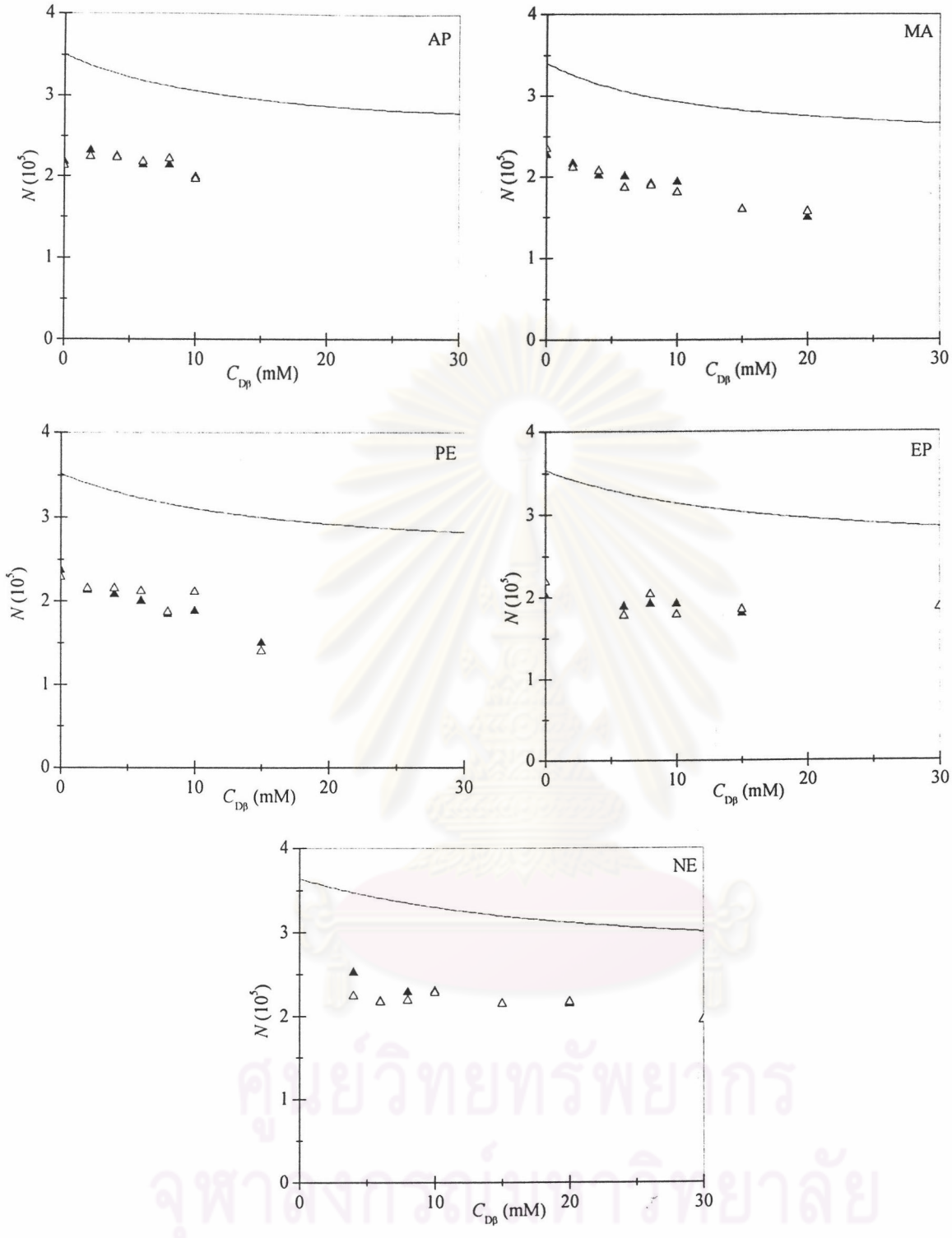

(a) fixed 8.0 mM C_β over a wide range of $C_{D\beta}$

Figure 3.19 Observed (symbols) and predicted (solid lines) peak efficiency (N) for each pair of AP, MA, PE, EP and NE enantiomers using dual cyclodextrins at fixed (a) 8.0 and (b) 10.0 mM C_β with a wide range of $C_{D\beta}$. ▲ and △ are the average for two enantiomers in the first and second run, respectively. ▲ and ∆ are the average for two enantiomers in the first and second run, respectively.

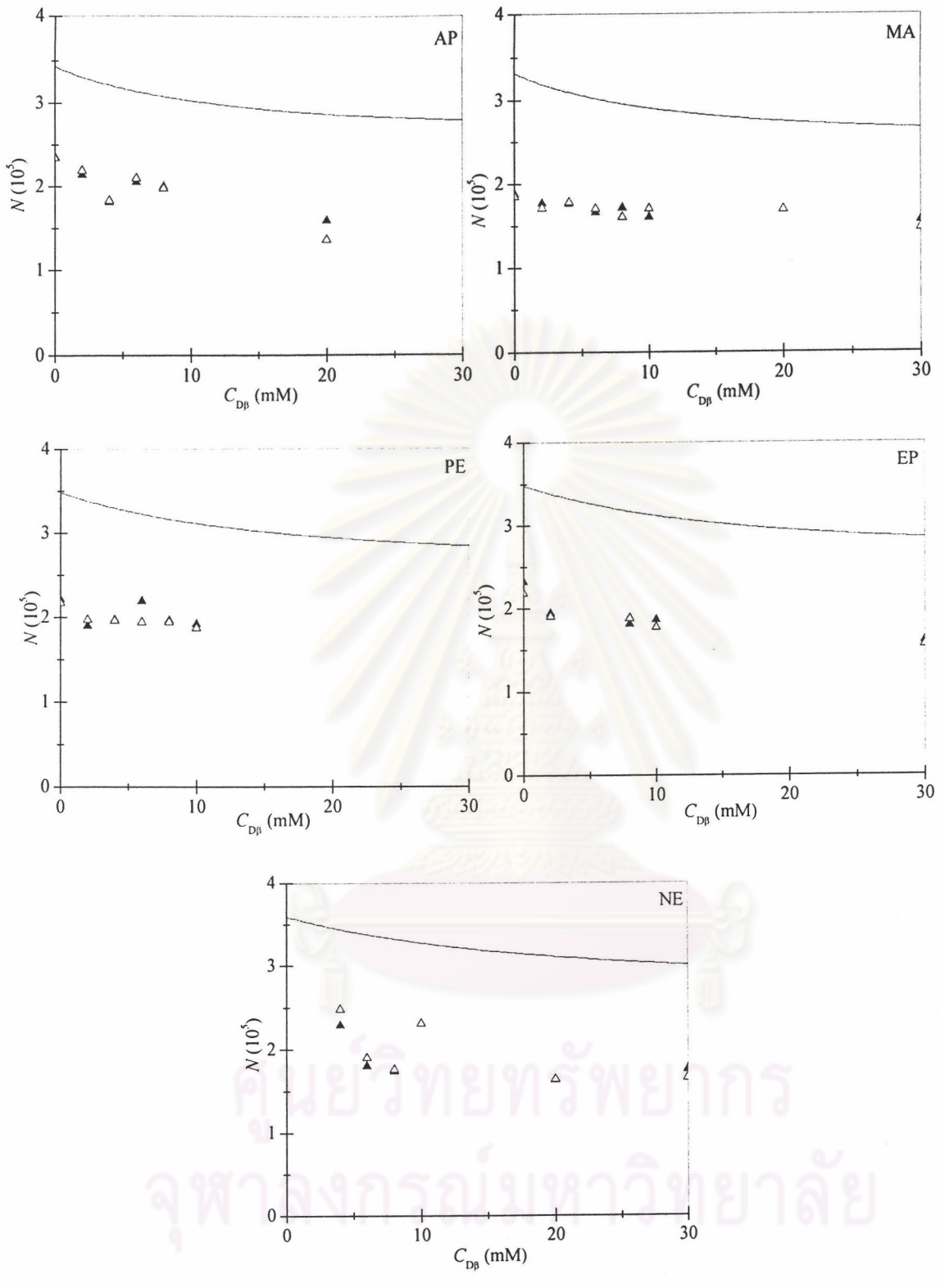

(b) fixed 10.0 mM C_β over a wide range of $C_{D\beta}$

Figure 3.19 Continued.

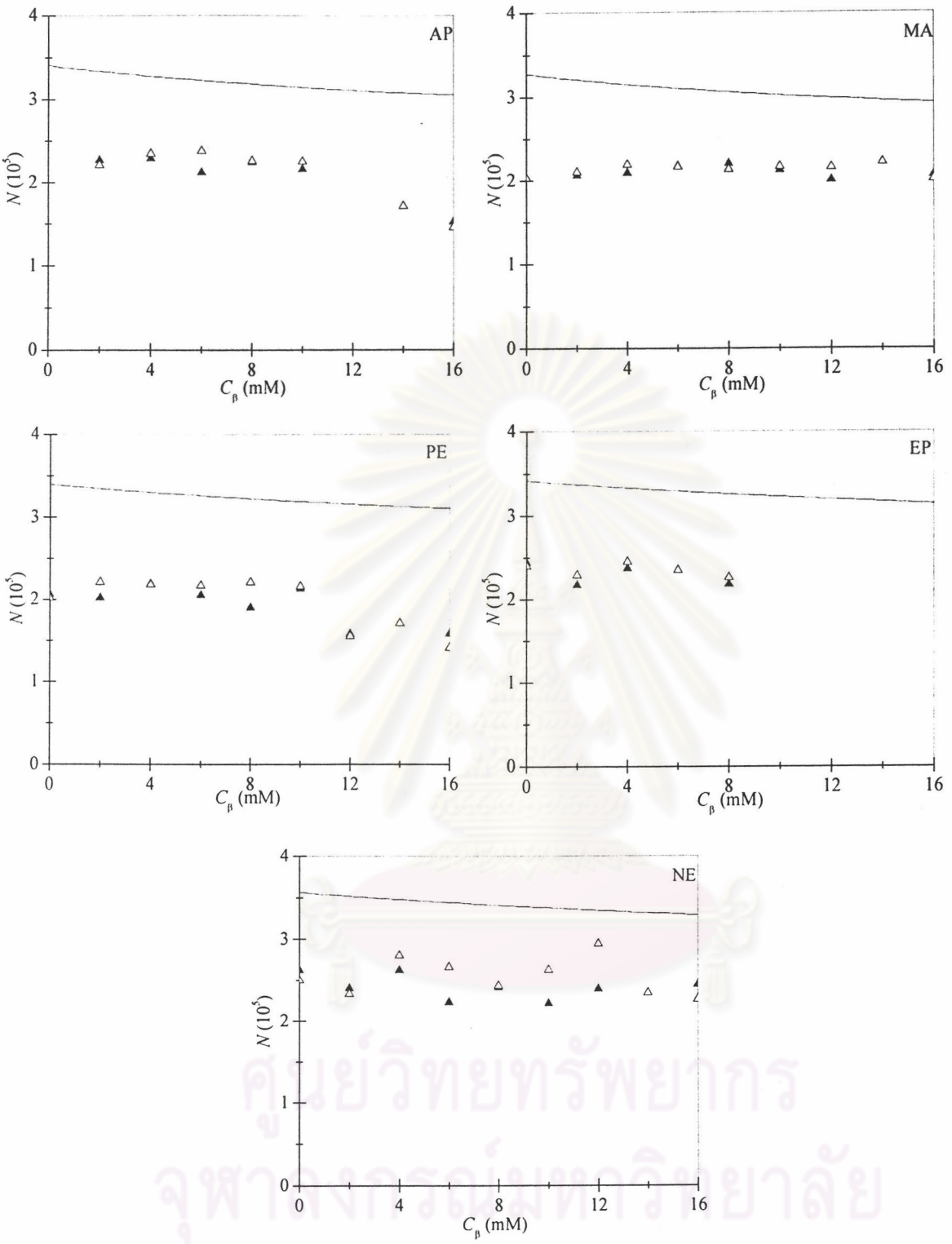

(a) fixed 6.0 mM $C_{D\beta}$ over a wide range of C_{β}

Figure 3.20 Observed (symbols) and predicted (solid lines) peak efficiency (N) for each pair of AP, MA, PE, EP and NE enantiomers using dual cyclodextrins at fixed (a) 6.0 and (b) 10.0 mM $C_{D\beta}$ with a wide range of C_{β}. ▲ and △ are the average for two enantiomers in the first and second run, respectively. ▲ and △ are the average for two enantiomers in the first and second run, respectively.

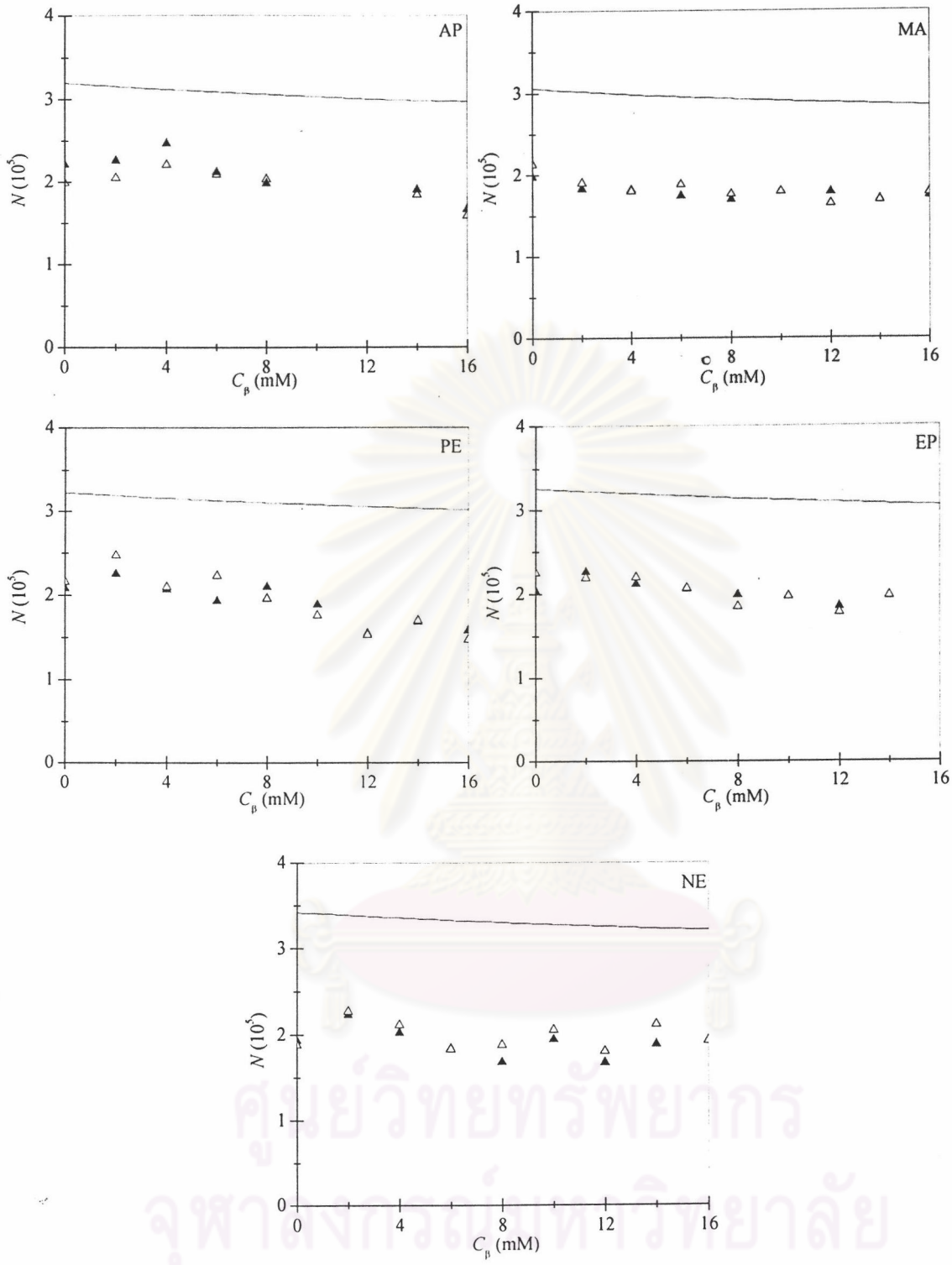

(b) fixed 10.0 mM $C_{D\beta}$ over a wide range of C_β

Figure 3.20 Continued.

3.2.5.4 Observed and Predicted Enantiomeric Resolution

Figure 3.21 shows a comparison of the values of observed and predicted resolution over a wide range of CD concentrations. The predicted values of R_s were calculated using Equation 3.12 and data of $\bar{\mu}$, $\Delta\mu$ and $\bar{N}$ in the dual CDs system. Over a wide range of CD concentrations, the observed and predicted values have the same trend. However, observed resolution slightly less than prediction was obtained due to observed less than predicted peak efficiency. Since R_s depends on $\Delta\mu$, a change in R_s of enantiomers in dual CDs can be explained using theoretical models of $\Delta\mu$ as previously discussed in Sections 3.33 and 3.34.

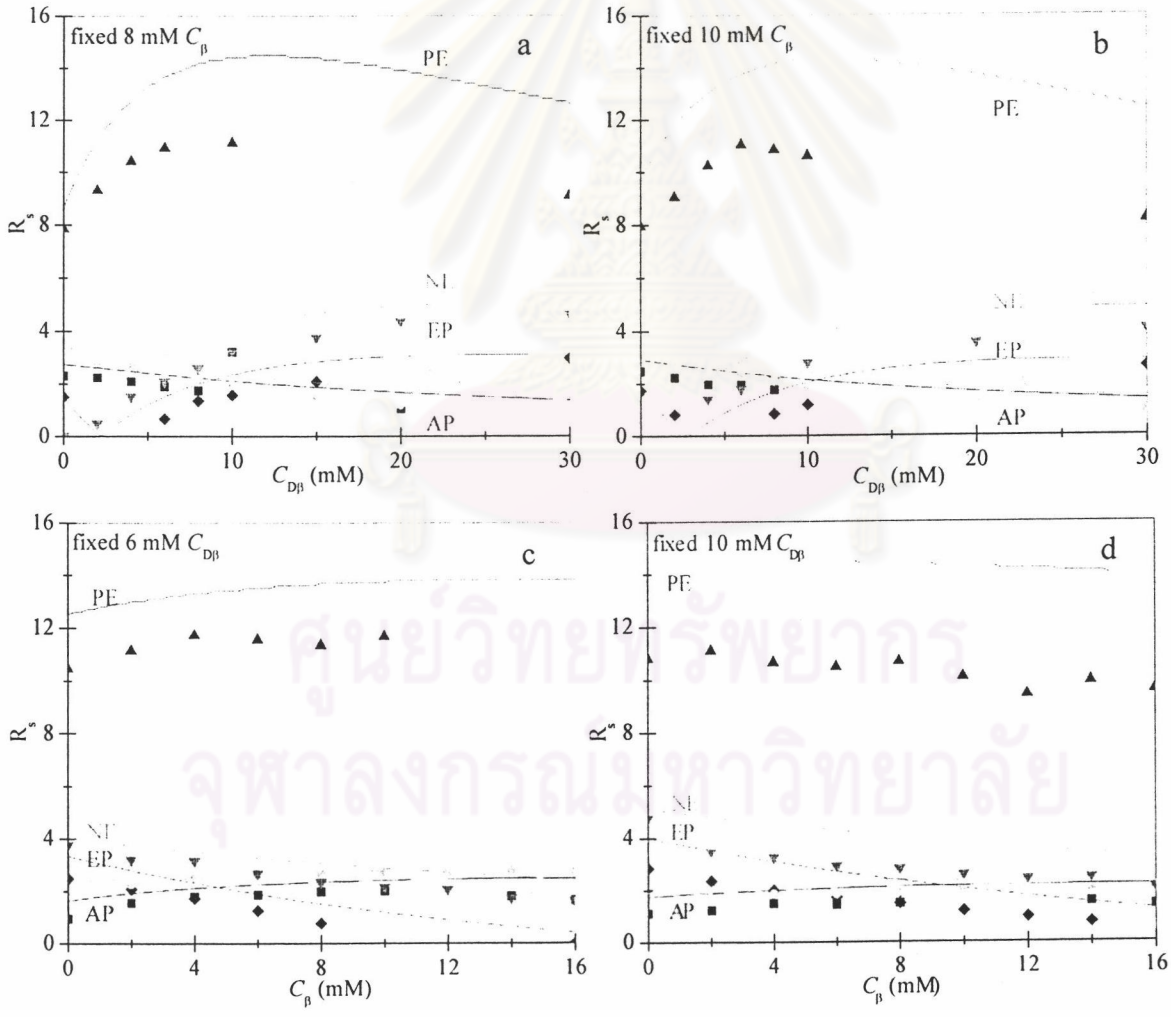

Figure 3.21 Observed (symbols) and predicted (solid lines) resolution (R_s) for each pair of AP, MA, PE, EP and NE enantiomers using dual cyclodextrins. Observed R_s is the average for two runs. ■: AP, ●: MA, ▲: PE, ◆: EP and ▼: NE. Observed and predicted values of R_s are obtained from Equation 3.12 and data from Figures 3.22 and 3.23.

3.2.6 Suitable Concentrations of Dual CDs for Simultaneous Separation of Several Pairs of Enantiomers

Figures 3.22 and 3.23 show plots of μ for each analyte in dual CDs at fixed C_β over various $C_{D\beta}$ and fixed $C_{D\beta}$ over various C_β, respectively, using Equations 3.16 and 3.17 and data in Table 3.1. It is seen that addition of CD2 in BGE containing CD1 affects on a change in μ of each isomer. This may result in overlapping some pairs of analytes.

From Figure 3.22a, at 10.0 mM β-CD without DM-β-CD, identical μ for NE enantiomers is due to its enantioselectivity of 1.0, as shown in Table 3.1. Addition of DM-β-CD resulted in an increase in Δμ of NE enantiomers due to α_α = 1.187 and Δμ model of Type I as shown in Table 3.6, but reversed migration order of EP enantiomers, leading to a decrease in Δμ of EP at $C_{D\beta}$ from 0 to 3.0 mM and an increase in Δμ at $C_{D\beta}$ above 3.0 mM. This is in agreement with electropherograms in Figure 3.12b. From Figures 3.14b and 3.21b, the observed and predicted values of Δμ and R_s decreased with an increase in $C_{D\beta}$. Predicted values of R_s in Figure 3.21b indicate that achieved baseline resolution (R_s > 1.5) for each pair of enantiomers should be obtained in a $C_{D\beta}$ range of 7.0 to 25.0 mM. However, observed values of R_s slightly less than 1.5 were obtained for EP enantiomers at 8.0 and 10.0 mM DM-β-CD, and for AP and MA enantiomers at $C_{D\beta}$ above 20.0 mM. In addition, electropherograms in Figure 3.12b show overlapped migration or co-migration of *R*-AP:(1*S*,2*S*)-PE at $C_{D\beta}$ above 4.0 mM and (1*R*,2*R*)-PE:(1*R*,2*S*)-EP at $C_{D\beta}$ above 10.0 mM. Therefore, achieved baseline resolution was not obtained for simultaneous separation of all test analytes using fixed 10.0 mM β-CD over DM-β-CD concentrations in a range of 0 to 30.0 mM.

Figure 3.22b, at 8.0 mM β-CD without DM-β-CD, indicate no separation of NE enantiomers and overlapped migration of three analytes (*S*-AP and EP enantiomers). This agrees with electropherograms in Figure 3.12a. Addition of DM-β-CD in the BGE containing fixed 8.0 or 10.0 mM β-CD resulted in same trend of a change in Δμ and R_s of enantiomers (Figures 3.14 and 3.21a-b). From electropherograms in Figure 3.12a and resolution in Figure 3.21a, at $C_{D\beta}$ of 2.0 and 4.0 mM, overlapped migration or co-migration was obtained for EP and NE enantiomers. At 6.0 mM $C_{D\beta}$, overlapped

migration of EP enantiomers was also observed. In addition, overlapped migration or co-migration of *R*-AP:(1*S*,2*S*)-PE at $C_{D\beta}$ above 10.0 mM and (1*R*,2*R*)-PE:(1*R*,2*S*)-EP at $C_{D\beta}$ above 15.0 mM. Therefore, addition of 8.0 mM DM-β-CD in the BGE containing fixed 8.0 mM β-CD gave simultaneous separation of all test analytes with achieved baseline resolution ($R_s > 1.5$), except for EP enantiomers having $R_s = 1.36$.

From Figures 3.13b, 3.21d and 3.23a, at 10.0 mM DM-β-CD without β-CD, R_s slightly less than 1.5 was obtained for the following pairs of analytes: (1*R*,2*R*)-PE:(1*R*,2*S*)-EP, (1*S*,2*R*)-EP:*S*-AP and *S*-AP:*R*-AP. Addition of β-CD up to 6.0 mM was found to improve R_s of these pairs. Worse resolution ($R_s < 1.5$) was observed for EP enantiomers and *R*-AP:(1*S*,2*S*)-PE at C_β above 10.0 and 8.0 mM, respectively. Therefore, addition of 6.0 mM β-CD in the BGE containing fixed 10.0 mM DM-β-CD gave simultaneous separation of all test analytes with achieved baseline resolution ($R_s > 1.5$).

Figures 3.13a, 3.21c and 3.23b, at 6.0 mM DM-β-CD without β-CD, showed co-migration (1*S*,2*R*)-EP:*R*-AP and overlapped migration of these two analytes with *S*-AP. Addition of β-CD up to 4.0 mM provided better R_s of these analytes. Poorer resolution ($R_s < 1.5$) was obtained for EP enantiomers and *R*-AP:(1*S*,2*S*)-PE at C_β above 6.0 and 10.0 mM, respectively. Therefore, addition of 4.0 mM β-CD in the BGE containing fixed 6.0 mM DM-β-CD gave simultaneous separation of all test analytes with achieved baseline resolution ($R_s > 1.5$).

It can be concluded from this section that the dual CDs containing 4.0 mM β-CD and 6.0 mM DM-β-CD was found to provide achieved baseline resolution of all test analytes, while a single CD of 10.0 mM β-CD gave no separation of NE enantiomers and partial separation of (1*R*,2*R*)-PE:(1*S*,2*R*)-EP and (1*R*,2*S*)-EP:*S*-AP, and a single CD of 10.0 mM DM-β-CD gave partial separation of; (1*R*,2*R*)-PE:(1*R*,2*S*)-EP, (1*S*,2*R*)-EP:*S*-AP and *S*-AP:*R*-AP enantiomers.